

# Deep inelastic scattering off a $\mathcal{N} = 4$ SYM plasma at strong coupling

---

**Y. Hatta and E. Iancu**

*Service de Physique Théorique, CEA Saclay, F-91191 Gif-sur-Yvette, France*  
*E-mail: Yoshitaka.Hatta@cea.fr, Edmond.Iancu@cea.fr*

**A. H. Mueller**

*Department of Physics, Columbia University, New York, NY 10027, USA*  
*E-mail: amh@phys.columbia.edu*

**ABSTRACT:** By using the AdS/CFT correspondence we study the deep inelastic scattering of an  $\mathcal{R}$ -current off a  $\mathcal{N} = 4$  supersymmetric Yang–Mills (SYM) plasma at finite temperature and strong coupling. Within the supergravity approximation valid when the number of colors is large, we compute the structure functions by solving Maxwell equations in the space–time geometry of the  $AdS_5$  black hole. We find a rather sharp transition between a low energy regime where the scattering is weak and quasi–elastic, and a high–energy regime where the current is completely absorbed. The critical energy for this transition determines the plasma saturation momentum in terms of its temperature  $T$  and the Bjorken  $x$  variable:  $Q_s = T/x$ . These results suggest a partonic picture for the plasma where all the partons have transverse momenta below the saturation momentum and occupation numbers of order one.

---

## Contents

<b>1. Introduction</b>	<b>1</b>
<b>2. General setup and basic equations</b>	<b>6</b>
<b>3. Low energy: the multiple scattering series</b>	<b>11</b>
<b>4. High energy: deep inelastic scattering</b>	<b>15</b>
<b>5. Saturation and the partonic structure of the plasma</b>	<b>18</b>
<b>A. Structure functions: Definitions and sum rules</b>	<b>24</b>
<b>B. Low energy: tunnel effect</b>	<b>25</b>
<b>C. The operator product expansion at weak coupling</b>	<b>28</b>
<b>D. High energy: the WKB approximation</b>	<b>30</b>

---

## 1. Introduction

Over the recent years, there has been increasing evidence, coming from the experimental results at RHIC and their theoretical interpretations [1, 2, 3, 4], and also from theoretical studies of the QCD thermodynamics [5, 6, 7], that the hadronic matter produced after a high-energy heavy ion collision may interact rather strongly, in spite of being in the deconfined phase of QCD and having a relatively high partonic density. For instance, the success of theoretical approaches based on hydrodynamics [3, 8], which assumes local thermal equilibrium and vanishing, or small, viscosity, in describing collective phenomena like elliptic flow [9, 10], suggests rapid thermalization and a low viscosity-to-entropy ratio for the matter produced at RHIC, which are hallmarks of a nearly-ideal fluid, with strong interactions. Also, the experimental results for the ‘jet-quenching parameter’ at RHIC [11, 12], which is a measure of the rate at which highly energetic partons lose energy in the surrounding medium, have been interpreted [13, 14] to yield values which are too large to be explained by weak coupling calculations [15, 16] (but this interpretation is not universally accepted; see, for instance, [17]). Furthermore, lattice studies of the QCD thermodynamics give evidence for a strong coupling behaviour (like the persistence of meson-like bound states [18, 19, 20, 21] and strong deviations from the pressure of an ideal gas of quarks and gluons [5, 6]) up to temperatures a few times the critical temperature for deconfinement. Such conclusions are corroborated by analytic calculations for the quark-gluon plasma showing that the weak-coupling expansion is too poorly convergent to be useful in practice for all temperatures of interest [22, 23, 24, 25].

These and similar observations have urged the need for non-perturbative studies of the hadronic matter at relativistically high temperatures and densities. While lattice gauge theory is a privileged tool to non-perturbatively address static properties like the thermodynamics or the screening masses, its extension towards dynamical problems, like transport phenomena, dispersion relations, or the high-energy scattering, remains prohibitively complicated, and new methods are therefore required to systematically address such problems at strong coupling. The AdS/CFT correspondence [26], although so far limited, in its most convincing formulation, to gauge theories which are ‘simpler’ (in the sense of having more symmetries) than QCD, is the most promising candidate in that sense.

This method can most easily deal with the large- $N$  limit, with  $N$  the number of colors, where the gauge coupling  $g$  is small but the ‘t Hooft coupling  $\lambda = g^2 N$  is large, in which case the  $\mathcal{N} = 4$  supersymmetric Yang–Mills (SYM) theory can be mapped onto a weakly-coupled string theory, that can be studied via semi-classical techniques. Leaving aside the structural differences between the  $\mathcal{N} = 4$  SYM theory, which is conformal, and real QCD — these differences can be argued to be less important in well-chosen physical regimes, and, besides, some of them can be incorporated into extensions of the  $\mathcal{N} = 4$  SYM theory (for which, however, the AdS/CFT correspondence is less firmly established) —, it is still not clear whether the aforementioned parametric conditions can be made consistent with the situation in QCD, where  $N = 3$  and  $g \sim \mathcal{O}(1)$  (giving  $\lambda \simeq 3 \div 6$ ) in the interesting physical regimes. But even if a detailed, quantitative, comparison to real QCD (in particular, to the experimental data) would be premature, it is nevertheless clear that the AdS/CFT approach can provide valuable information about the non-perturbative behaviour of gauge theories, which should allow us to better constraint the physical reality of QCD from the strong-coupling end.

Given these promising features, and the experimental imperatives at RHIC or LHC, it is not surprising that, over the last few years, there was a profusion of applications of the AdS/CFT techniques to problems of interest for high-density QCD. Following early applications to thermodynamics [27, 28] and the pioneering calculation, by Policastro, Son, and Starinets, of the shear viscosity [29, 30], there was an intense activity towards computing the jet-quenching parameter [31, 32, 33, 34], the energy-loss of a heavy quark [35, 36, 37, 38] or of a quark–antiquark pair [39, 40, 41, 42, 43, 44], the diffusion rate for a heavy quark [45, 46], the energy disturbances due to moving quarks [47, 48], the Debye screening mass [49, 50], the production rate for photons and dileptons [51], or the Bjorken expansion and the approach towards thermalization [52, 53, 54, 55] — all of that in the context of the strongly-coupled  $\mathcal{N} = 4$  SYM plasma at finite temperature (sometimes extended to include a chemical potential).

Several of the studies mentioned above have been concerned with the long-range ( $\Delta x \gg 1/T$ ) or large-time ( $\Delta t \gg 1/T$ ) behaviour of the strongly-coupled plasma, as relevant e.g. for hydrodynamics, thermalization, or transport phenomena. On the other hand, in order to study the propagation of ‘hard’ (i.e., highly energetic and relatively small) probes through the plasma, like jets or electromagnetic probes, it is essential to have a good understanding of the plasma structure on *short* space-time separations  $\ll 1/T$ , much alike the parton picture in perturbative QCD. Of course, at strong coupling there is *a priori* not clear whether the notion of a ‘parton’ — in the sense of a point-like constituent which behaves as quasi-free during the interaction with the external probe — makes sense in the first place, neither if such a ‘parton’, in case it exists,

should belong to an individual ‘quasiparticle’ (a thermal excitations with energies and momenta of order  $T$ ), or rather is a property of the plasma as a whole. In other terms, is the partonic distribution of the plasma (again, assuming that this exists) the direct sum of the respective distributions for the constituent quasiparticles, with appropriate thermal weights, or rather is this qualitatively different ?

Such questions are extremely difficult and below we shall not attempt to answer them in full generality. In particular, it is not yet understood whether a strongly-coupled gauge plasma admits a quasiparticle picture on the thermal scale  $1/T$ , so like the Landau theory of a Fermi liquid, or the quasiparticle structure of the quark-gluon plasma emerging from resummations of perturbation theory [56, 7]. Fortunately, however, there is no need to properly understand the structure of the plasma on this scale  $1/T$  so long as we are merely interested on the corresponding structure on much shorter space-time scales  $\ll 1/T$ . Indeed, the latter can be directly measured (at least, in a Gedankenexperiment) by an external probe with high energy and momentum ( $\omega, q \gg T$ ). From the experience with QCD we know that the most convenient measurement of that type — that whose results are most directly related to the parton structure of the target — is the ‘deep inelastic scattering’ (DIS) of a leptonic probe off the plasma.

DIS at strong coupling in the context of the AdS/CFT correspondence has been so far considered [57, 58] only for the case where the target is a single hadron (a ‘dilaton’). In this approach, the ‘electromagnetic’ probe which initiates the scattering is the conserved current associated with a particular  $U(1)$  symmetry (the ‘ $\mathcal{R}$ -current’), whose associated ‘ $\mathcal{R}$ -charge’ is also carried by the light degrees of freedom which are present inside the hadrons. By computing the current-current correlator in the hadron wavefunction, one can extract the same information about hadronic structure functions that would be obtained by DIS via a ‘photon’ coupled to the  $U(1)$  current. In terms of the standard kinematical variables  $Q^2$  and  $x$ , with  $Q^2 = q^2 - \omega^2$  the virtuality of the current and  $x \approx Q^2/s$  (at high energy  $s \gg Q^2$ ), the DIS structure function  $F_2(x, Q^2)$  is a measure of the number of partons which carry a longitudinal momentum fraction  $x$  and occupy an area  $\sim 1/Q^2$  in the transverse, impact parameter, space.

In this paper, we shall use the same general setup — the scattering between the  $\mathcal{R}$ -current and the plasma — to compute the structure functions of a strongly-coupled  $\mathcal{N}=4$  SYM plasma at finite temperature. It turns that, in this case, the formalism is quite different — in fact, somewhat simpler and also conceptually clearer — than in the case of a single-hadron target considered in Ref. [57, 58]. There are several reasons for such differences:

First, the string theory dual of the  $\mathcal{N}=4$  SYM plasma is unambiguously known, at the level of the original formulation of the AdS/CFT correspondence [26] : this is a ‘black-hole’ (more precisely, a non-extremal black three-brane; see Sect. 2 below for details) in a curved space-time geometry which is asymptotically  $AdS_5 \times S^5$ . By contrast, in order to accommodate a hadronic state, the  $\mathcal{N}=4$  SYM theory (which has no confinement) must be ‘deformed’ in the infrared, in such a way to break down conformal symmetry. This deformation is not unique and, besides, its dual analog in the string theory is generally ambiguous.

Second, the interplay between the large- $N$  limit and the high-energy limit turns out to be much more subtle for a single-hadron target than for a plasma. This is in turn related to an essential feature of the strong-coupling problem, which is the deep connection between the distribution of partons and the issue of unitarity in DIS at high energy. As explained in Ref.

[58], at strong coupling, most of the partons are concentrated in the kinematical region where the scattering is strong and the unitarity corrections are important (the analog of the ‘saturation’, or ‘color glass condensate’, region of perturbative QCD [59]). This is an important point that we shall try to motivate here via general arguments, and for which the subsequent calculations in this paper will provide an explicit realization:

One can heuristically understand this point by extrapolating the picture of parton evolution in perturbation theory: Partons at large  $x$  tend to radiate and thus drop down at smaller values of  $x$ . At weak coupling, the emitted partons are predominantly soft (i.e., they carry only a tiny fraction  $x' \ll 1$  of the longitudinal momentum of their parent partons), so, even for very high energies, there is still a substantial fraction of the parton distribution at relatively large values of  $x$ . These large- $x$  partons carry almost all of the hadron energy and momentum, but they are unimportant for high-energy scattering, which is rather controlled by the bulk of the distribution at small- $x$ . At strong coupling, on the other hand, there is no penalty for the hard emissions; the distribution of the energy among the child partons after a branching is essentially democratic, and hence the overall distribution can very fast degrade, via successive branchings, down to very small values of  $x$ . One therefore expects the structure functions at strong coupling to be concentrated at small values of  $x$ , but the question is, how small? These functions are, of course, constrained by energy-momentum conservation — the small- $x$  partons must carry the overall energy and momentum of the hadron —, but this constraint (a ‘sum-rule’ on  $F_2$ ) is not sufficient to determine the parton distribution. A more severe constraint comes from unitarity: in the kinematical region where the scattering is strong, in the sense that the scattering amplitude has reached the unitarity bound, the structure functions are, by definition, large, and hence the partons exist. Thus, at strong coupling, the search for the parton distribution is tantamount to understanding the unitarity problem for DIS.

This is where the large- $N$  limit becomes important: the elementary scattering amplitude is suppressed<sup>1</sup> by a factor  $1/N^2$ , so for a *single-hadron target* and in the strict large- $N$  limit ( $N \rightarrow \infty$  at fixed energy), the scattering can never become strong, and thus the bulk of the partons cannot be seen. This is the situation considered in Ref. [57], and indeed it has been found there that the dilaton has no point-like constituents except at extremely small values of  $x$  (for a given resolution  $Q^2$ ), within a kinematical domain which squeezes exponentially to zero when increasing  $\lambda$ .

But the partonic structure of the dilaton reveals itself after relaxing the large- $N$  limit, as we did in Ref. [58]. Namely, we found that, for sufficiently large  $Q^2$ , the partons are all located in the strong-scattering region at  $x \lesssim x_s(Q^2)$ , where  $x_s(Q^2) \simeq \Lambda^2/(N^2 Q^2)$  is the ‘saturation line’ (a line in the kinematical plane  $(x, Q^2)$  along which the elementary amplitude is constant and of order one) and  $\Lambda$  is the infrared cutoff which fixes the size of the dilaton. Moreover, the phase-space distribution of these partons turns out to be remarkably simple (and somehow reminiscent of the gluon distribution in the ‘color glass condensate’ at weak coupling [59]): there is essentially a single parton of a given color per unit cell in phase-space. This *a posteriori* legitimates the use of the ‘electromagnetic’ current as a probe of the parton distribution: in spite of the coupling being strong, the current can interact only with one parton at a time, and thus

---

<sup>1</sup>There is no similar suppression for the DIS structure functions because the strength  $J^2$  of the  $\mathcal{R}$ -current increases like  $N^2$ , due to the color degrees of freedom of the fields which make up the current.

it can faithfully measure the parton number. Since, moreover, partons with very small  $x \ll x_s$  carry only little energy and momentum, it is clear that the hadron total energy and momentum is concentrated in the partons near the saturation line  $x = x_s(Q^2)$ .

Returning, after this long digression, to the plasma problem of current interest, we note that in this context one can simplify the problem by using the large- $N$  approximation without losing the salient features: for a plasma target, the scattering can be strong even in the large- $N$  limit, because the plasma involves  $N^2$  degrees of freedom per unit volume — as manifest from the fact that its entropy density scales like  $N^2 T^3$  [27, 28] —, which compensates for the  $1/N^2$  suppression of the elementary scattering amplitude. Note that, at this point, and at several other places in the paper, we use a heuristic language in which the plasma thermal degrees of freedom are treated as ‘quasiparticles’ with typical energies and momenta of order  $T$ , and the overall scattering process is viewed as the sum of elementary scatterings between these quasiparticles and the  $\mathcal{R}$ -current. This language, inspired by the situation at weak coupling, is admittedly ambiguous at strong coupling, and is used here only to gain more intuition into mathematical manipulations which by themselves are free of any ambiguity.

Specifically, in the large- $N$  limit of interest, the scattering between the  $\mathcal{R}$ -current and the plasma can be described in the supergravity approximation, as the propagation of the gravitational perturbation induced by the current in the background metric of the black three-brane. The current-current correlator relevant to DIS is then computed from the action evaluated on the solution to the classical wave equation — an imaginary part in this solution being synonymous of inelasticity in the scattering of the current. The wave dynamics is non-trivial in only one dimension — the radial dimension of  $AdS_5$ , which plays the role of an ‘impact parameter’ between the current and the black hole. The relevant wave equation can be formally rewritten as a Schrödinger equation in one spatial dimension (actually, two such equations, for the longitudinal and transverse waves, respectively). Then, the dynamics is controlled by the potential in this equation and, more precisely, by the competition between two important terms: a ‘repulsive’ term proportional to  $Q^2$  which by itself would keep the wave at the boundary of  $AdS_5$  (far away from the horizon of the black hole), and an ‘attractive’ term, proportional to the energy times the temperature, which tends to pull the wave towards the black hole. We thus distinguish between two physical regimes:

(i) At relatively low energy and/or low temperature, such that  $x \gg T/Q$ , the repulsive term dominates, and the wave remains confined near the boundary. (For DIS off the plasma,  $x \sim Q^2/qT$ , and we recall that  $T/Q \ll 1$  for the physical problem of interest.) In this regime the scattering is weak and quasi-elastic (the imaginary part in the classical solution is extremely small, since generated via tunneling through the potential). Correspondingly, the DIS structure functions are exponentially small, e.g.,  $F_2 \sim \exp\{-c(xQ/T)^{1/2}\}$ , a result that we interpret as the absence of point-like constituents in the SYM plasma having  $x \gg T/Q$ .

(ii) At high enough energy, such that  $x \lesssim x_s(Q) \simeq T/Q$ , the attractive term in the potential takes over, and then the wave escapes inside the bulk of  $AdS_5$ , until it gets absorbed by the black hole. This absorption generates a large imaginary part in the solution, and hence a large contribution to the structure functions for DIS, which for  $x \sim x_s$  is evaluated as  $F_2 \sim N^2 T Q$  (see Sect. 4 for more general results). These results for the structure functions represent the unitarity limit for the current-plasma scattering, which in this case is saturated by the complete

absorption of the current — a genuine ‘black disk’ limit.

The physical interpretation of these results at small  $x$  in terms of partons in the plasma requires some care: the plasma being infinite, one needs to take into account the finite duration of the interaction, and also make a boost to a Lorentz frame where the notion of a parton makes sense (all the other calculations being done in the plasma rest frame). But after this is properly into account, it becomes clear that our results have a natural partonic interpretation, which moreover is consistent with the corresponding picture for a hadron, as obtained in Ref. [58]. Namely, for a given resolution  $Q^2$ , the partons exist only at sufficiently small values of  $x$ , such that  $x \lesssim T/Q$ , and are homogeneously distributed in the three-dimensional phase-space, with occupation numbers of order one. Equivalently, for a given value of  $x$ , partons exist only at transverse momenta smaller than, or equal to, the saturation momentum  $Q_s(x) \simeq T/x$ . This value for the saturation momentum is consistent with the representation of the  $\mathcal{N} = 4$  SYM plasma as an incoherent superposition of thermal quasiparticles.

It is finally interesting to notice a similarity between our above estimate for the plasma saturation momentum and some results in the literature [40, 41] for the *screening length*  $L_s(v, T)$  of a heavy quark–antiquark pair moving at velocity  $v$  in the hot  $\mathcal{N} = 4$  SYM plasma. The screening length is the maximal separation for which the quark and the antiquark can be still connected by a string ‘hanging down’ in the radial direction of  $AdS_5$ . In Refs. [40, 41], one found  $L_s(v, T) \simeq \kappa(1 - v^2)^{1/4}/T$  with  $\kappa$  a numerical constant (at least for  $v$  close to 1). Now, in the analogy with our DIS problem, the ‘quark–antiquark pair’ of Refs. [40, 41] corresponds to the SYM system emerging from the  $\mathcal{R}$ -current, which has a typical transverse extent  $1/Q$  and a rapidity  $q/Q$ . It is therefore natural to identify our variables  $1/Q$  and  $q/Q$  with the size  $L$  and the Lorentz gamma factor  $\gamma = 1/\sqrt{1 - v^2}$  of the  $q\bar{q}$  pair, respectively. In particular our saturation momentum  $Q_s(x, T)$  should be compared to the inverse screening length  $1/L_s(v, T)$ . To that aim, it is preferable to rewrite the result in Refs. [40, 41] as  $1/L_s^2 \sim \gamma T^2$ ; after replacing  $1/L_s \rightarrow Q_s$  and  $\gamma \rightarrow q/Q_s$ , this translates into  $Q_s^3(q, T) \sim qT^2$ , which is parametrically the same as our result for  $Q_s$ , as alluded to above. It would be interesting to explore this correspondence in more detail.

## 2. General setup and basic equations

Following the general strategy with the problem of deep inelastic scattering, our objective will be to compute the retarded current–current commutator

$$R_{\mu\nu}(q) = i \int d^4x e^{-iq \cdot x} \theta(x_0) \langle [J_\mu(x), J_\nu(0)] \rangle, \quad (2.1)$$

whose imaginary part determines the DIS structure functions. In the present context, the density  $J_\mu(x)$  which enters Eq. (2.1) refers to an  $\mathcal{R}$ -current — the conserved current associated with a gauged  $U(1)$  subgroup of the  $SU(4)$  global  $\mathcal{R}$ -symmetry —, and the expectation value is understood as a thermal average, over the statistical ensemble corresponding to a  $\mathcal{N} = 4$  SYM plasma at temperature  $T$ . The operator  $J_\mu(x)$  for the  $\mathcal{R}$ -current receives contributions from the fermionic and scalar fields of the  $\mathcal{N} = 4$  SYM theory. Accordingly, and following the example of perturbative QCD, we expect the imaginary part of  $R_{\mu\nu}(q)$  to give us information about the constituents of the finite-temperature plasma, just as the structure function of the proton gives information on its (partonic) structure in perturbative QCD.

In the limit where the Yang–Mills coupling  $g^2$  is small but the ‘t Hooft coupling  $\lambda = g^2 N$  is large, the AdS/CFT correspondence allows one to evaluate Eq. (2.1) in terms of classical supergravity in the metric of the  $AdS_5 \times S^5$  black hole. The corresponding metric reads

$$ds^2 = \frac{(\pi T R)^2}{u} (-f(u) dt^2 + d\mathbf{x}^2) + \frac{R^2}{4u^2 f(u)} du^2 + R^2 d\Omega_5^2, \quad (2.2)$$

where  $T$  is the temperature of the black hole (the same as for the  $\mathcal{N} = 4$  SYM plasma),  $R$  is the common radius of  $AdS_5$  and  $S^5$ ,  $t$  and  $\mathbf{x} = (x, y, z)$  are the time and, respectively, spatial coordinates of the physical Minkowski world,  $u$  is the radial coordinate on  $AdS_5$ ,  $d\Omega_5^2$  is the angular measure on  $S^5$ , and  $f(u) = 1 - u^2$ . Note that our radial coordinate has been rescaled in such a way to be dimensionless: in terms of the more standard, dimensionfull, coordinate  $r$ , it reads  $u \equiv (r_0/r)^2$ , with  $r_0 = \pi R^2 T$ . Hence, in our conventions, the black hole horizon lies at  $u = 1$  and the Minkowski boundary at  $u = 0$ .

In order to evaluate Eq. (2.1), one needs to study the metric perturbation induced by the  $R$ -current  $J_\mu$  around the background metric (2.2). The relevant gravitational wave is a vector field  $A_m(t, \mathbf{x}, u)$  in  $AdS_5$ , which obeys the classical equations of motion with given boundary conditions at  $u = 0$ . (Here,  $m = \mu$  or  $u$  is the coordinate index on  $AdS_5$ , with  $\mu = 0, 1, 2, 3$  referring to a Minkowski coordinate.) Once the corresponding solution is known, the tensor  $R_{\mu\nu}$  can be extracted from the classical supergravity action evaluated as a functional of the boundary fields  $A_\mu(t, \mathbf{x}, 0)$  (see below). We shall assume the external current to be weak, so that the metric perturbations be small and the corresponding equations be linear in  $A_m$ . Accordingly, we only need the supergravity action to quadratic order in  $A_m$ , which reads (see, e.g., [64])

$$S = -\frac{N^2}{64\pi^2 R} \int d^4x du \sqrt{-g} g^{mp} g^{nq} F_{mn} F_{pq}, \quad (2.3)$$

where  $F_{mn} = \partial_m A_n - \partial_n A_m$ ,  $\partial_m = \partial/\partial x^m$  with  $x^m = (t, \mathbf{x}, u)$ , and  $g = \det(g_{mn})$ . The classical equations of motion generated by the action (2.3) are the Maxwell equations in the geometry of the  $AdS_5$  black hole. We shall work in the gauge  $A_u = 0$  and choose the incoming perturbation as a plane wave propagating in the  $z$  direction:  $q^\mu = (\omega, 0, 0, q)$ . Then we can write

$$A_\mu(t, \mathbf{x}, u) = e^{-i\omega t + iqz} A_\mu(u) \quad (2.4)$$

with the fields  $A_\mu(u)$  obeying the following equations (below,  $i = 1, 2$ )

$$\varpi A'_0 + k f A'_3 = 0 \quad (2.5)$$

$$A''_i + \frac{f'}{f} A'_i + \frac{\varpi^2 - k^2 f}{u f^2} A_i = 0 \quad (2.6)$$

$$A''_0 - \frac{1}{u f} (k^2 A_0 + \varpi k A_3) = 0 \quad (2.7)$$

where a prime on a field indicates a  $u$ -derivative and we have introduced dimensionless, energy and longitudinal momentum, variables, defined as

$$\varpi \equiv \frac{\omega}{2\pi T}, \quad k \equiv \frac{q}{2\pi T}. \quad (2.8)$$

Denoting  $a(u) \equiv A'_0(u)$ , Eqs. (2.5) and (2.7) can be combined to give

$$a'' + \frac{(uf)'}{uf} a' + \frac{\varpi^2 - k^2 f}{uf^2} a = 0, \quad (2.9)$$

which will be one of our key equations in what follows (the other one being Eq. (2.6) for  $A_i$ ).

The above equations (2.5)–(2.9) have already been presented in the literature (see, e.g., Refs. [60, 61, 62, 63, 64]), but in relation with other physical problems, corresponding to physical regimes very different from ours. These equations must be solved with the condition that the fields take generic values  $A_\mu = A_\mu(u=0)$  at the  $AdS_5$  boundary  $u=0$ . Then Eq. (2.7) implies the following boundary condition for  $a(u)$

$$\lim_{u \rightarrow 0} [ua'(u)] = k(kA_0 + \varpi A_3)|_{u=0} \equiv k^2 \mathcal{A}_L(0). \quad (2.10)$$

For the solutions to be uniquely specified, an additional boundary condition is still needed. Following Refs. [61, 64], we shall require the solution to be a purely outgoing wave near the horizon at  $u=1$ , where by ‘outgoing’ we mean a wave which is impinging into the black hole (and thus is departing from the Minkowski boundary). Physically, this corresponds to the fact that a wave cannot be reflected by the black hole, but only absorbed. Notice that, in the zero-temperature case where there is no black hole and the coordinate  $u$  extends to infinity, the corresponding boundary condition is simply that the fields be regular at  $u \rightarrow \infty$ .

Once the classical solution is known, the next step is to compute the corresponding, ‘on-shell’, value of the action. Starting with Eq. (2.3) and using the equations of motion to perform the integration over  $u$ , it is straightforward to deduce

$$S = -\frac{N^2 T^2}{16} \int d^4x \left[ \left( A_0 + \frac{\varpi}{k} A_3 \right) a(u) - A_i \partial_u A_i(u) \right]_{u=0}, \quad (2.11)$$

where we have dropped a contribution coming from  $u=1$  in accordance with the prescription in Ref. [61, 62]. Note that the appearance of the factor  $T^2$  in front of  $S$  is merely a consequence of our definition of the variable  $u$  (which scales like  $T^2$ , so  $\partial_u \sim 1/T^2$ ). If one returns to the dimensionfull radial coordinate  $r$ , then there is no apparent factor  $T^2$ , and indeed Eq. (2.11) has a non-trivial limit as  $T \rightarrow 0$ , corresponding to the vacuum polarization tensor for the  $\mathcal{R}$ -current (see Sect. 3). Given the plane-wave structure in Eq. (2.4), the action density in Eq. (2.11) is independent of  $x^\mu = (t, \mathbf{x})$ , so it is convenient to separate out the volume of space-time:  $S = \int d^4x \mathcal{S}$ . From the action density  $\mathcal{S}$ , the tensor  $R_{\mu\nu}(q)$  is finally obtained as

$$R_{\mu\nu}(q) = \frac{\partial^2 \mathcal{S}}{\partial A_\mu \partial A_\nu}, \quad (2.12)$$

where  $A_\mu \equiv A_\mu(u=0)$ . Note that the ensuing tensor has mass dimension two, as it should.

The tensor  $R_{\mu\nu}$  can be given the standard tensorial decomposition (see Appendix A), which shows that there are only two independent scalar components,  $R_1$  and  $R_2$ , whose imaginary parts determine the two DIS structure functions,  $F_1$  and  $F_2$ . (The precise definitions are given in Appendix A.) Since in practice we shall solve second-order differential equations with *real* coefficients, cf. Eqs. (2.6) and (2.9), it is interesting to understand how an *imaginary* part in the respective solutions (and hence a non-vanishing contribution to the DIS structure functions)

can arise in the first place. This is generated via the aforementioned boundary condition near  $u = 1$ , which allows for the absorption of the gravitational wave by the black hole.

For a given temperature  $T$  of the target plasma, the scalar functions  $R_i$ , or  $F_i$ , with  $i = 1, 2$ , depend in general upon two kinematical invariants, that we shall conveniently choose as the virtuality  $Q^2$  of the  $\mathcal{R}$ -current and the Bjorken  $x$  variable. These are defined as

$$Q^2 \equiv q^2 - \omega^2, \quad x \equiv \frac{Q^2}{-2(q \cdot n)T} = \frac{Q^2}{2\omega T}, \quad (2.13)$$

where  $n^\mu$  is the four-velocity of the plasma in a generic frame, and the second expression for  $x$  holds in the plasma rest frame, for which  $n^\mu = (1, 0, 0, 0)$ . Unless otherwise specified, in what follows we shall always work in the plasma rest frame. We shall consider the large- $Q^2$  and high-energy kinematics, where  $q^2 \gg Q^2 \gg T^2$  and hence  $\omega \simeq q$ . These conditions allow for both small ( $x \ll 1$ ) and large ( $x \sim \mathcal{O}(1)$ ) values of  $x$ , but in what follows we shall be mostly interested in small- $x$  regime where  $q \gg Q^2/T$ .

To conclude this section, let us present an alternative form for our key equations, (2.6) and (2.9), which is more insightful and also better suited for constructing approximate solutions via WKB techniques. Via simple manipulations, these equations can be brought into the form of the (time-independent) Schrödinger equation in one spatial dimension, that is,  $\psi'' - V\psi = 0$ .

Consider first Eq. (2.9): when rewritten for the new field  $\psi(u) \equiv \sqrt{u(1-u^2)} a(u)$ , this takes the form (with  $K^2 \equiv k^2 - \varpi^2$ )

$$\psi'' - \frac{1}{u(1-u^2)^2} \left[ -\frac{1}{4u}(1+6u^2-3u^4) + K^2 - k^2u^2 \right] \psi = 0, \quad (2.14)$$

which is of the Schrödinger type, as anticipated. In the interesting regime at  $k^2 \gg K^2 \gg 1$ , the potential  $V(u)$  in (2.14) is well approximated by

$$V = \frac{1}{u(1-u^2)^2} \left[ -\frac{1}{4u} + K^2 - k^2u^2 \right]. \quad (2.15)$$

This describes a potential barrier, whose shape is illustrated in Fig.1, and also in Fig. 2a, for three different physical situations, corresponding to different regimes for the ratio  $k/K^3$ : (i)  $k/K^3 < 8/(3\sqrt{3})$  in Fig.1a, (ii)  $k/K^3 = 8/(3\sqrt{3})$  in Fig.1b, and (iii)  $k/K^3 > 8/(3\sqrt{3})$  in Fig.1c. As it should be clear from Fig.1b, the critical value  $k/K^3 = 8/(3\sqrt{3})$  corresponds to the case where the height of the potential vanishes at its peak. Note that a value of  $\mathcal{O}(1)$  for the ratio  $k/K^3$  corresponds to a value  $x \sim T/Q \ll 1$  for the Bjorken variable.

We can understand much about the solution to (2.14) by inspection of these figures: When  $k/K^3 < 8/(3\sqrt{3})$  (the situation at intermediate energies), there is a high potential barrier (cf. Fig.1a), with classical turning points  $u_1 \simeq 1/(4K^2)$  and  $u_2 \simeq K/k$ . (Note that  $u_1 \ll u_2 \ll 1$  in the interesting regime where  $k \gg K \gg 1$ , with  $k \ll K^3$  though.) We then expect the solution  $\psi(u)$  to be concentrated within the classically allowed region at  $u \lesssim 1/K^2$ . Moreover, the DIS structure functions are expected to be extremely small in this case, since an imaginary part in the classical solution can develop only via tunneling through the high potential barrier.

On the other hand when  $k/K^3 > 8/(3\sqrt{3})$  (the high-energy case, cf. Fig.1c), there is no potential barrier any longer, so the gravitational wave can easily flow into the black hole and thus get absorbed by the latter. We then expect a large imaginary part to  $R_{\mu\nu}$ .

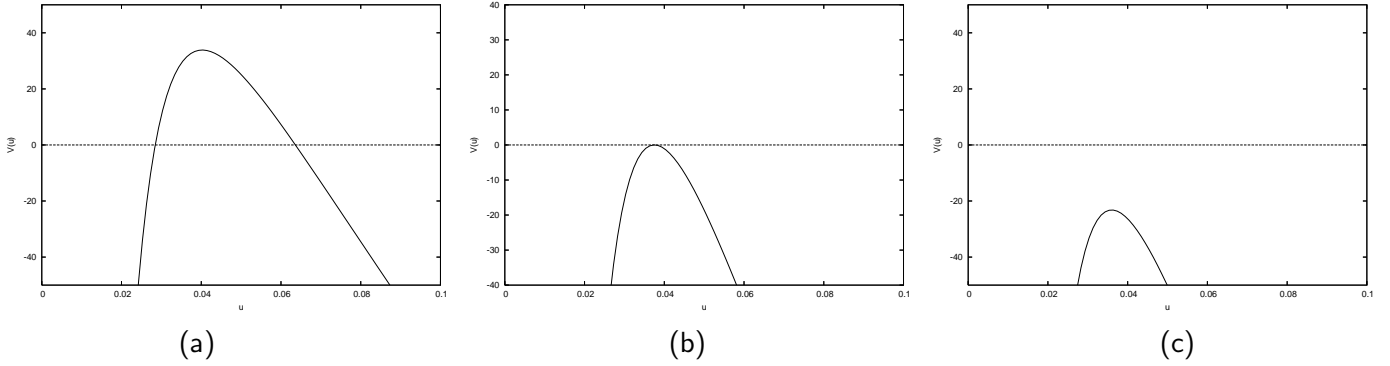


**Figure 1:**

The potential  $V(u)$  in Eq. (2.15) for three values of the ratio  $k/K^3$ : (a)  $k/K^3 < 8/(3\sqrt{3})$ , (b)  $k/K^3 = 8/(3\sqrt{3})$ , and (c)  $k/K^3 > 8/(3\sqrt{3})$ . For the figures to look more suggestive, all the chosen values for  $k/K^3$  are relatively close to the critical value  $8/(3\sqrt{3})$ .

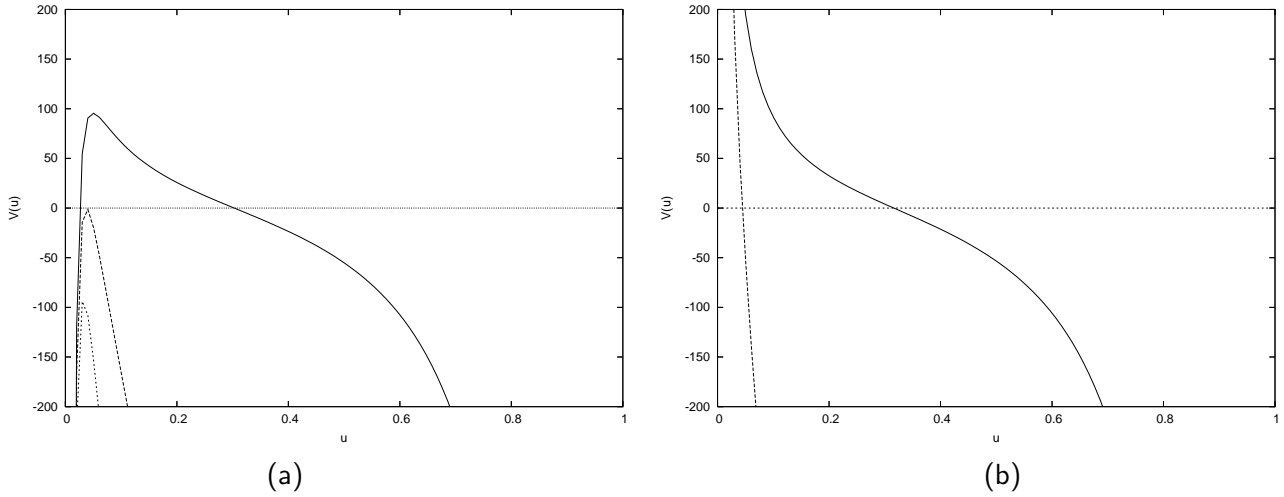


**Figure 2:**

The potentials  $V(u)$  corresponding to longitudinal waves, cf. Eq. (2.15) (left) and, respectively, transverse waves, cf. Eq. (2.17) (right), are represented for several values of the ratio  $k/K^3$ , corresponding to physical regimes well separated from each other.

Similar conclusions apply to the transverse modes  $A_i$  as well, although the corresponding argument is slightly more involved, and perhaps less intuitive. With the substitution  $\phi(u) \equiv \sqrt{(1-u^2)} A_i(u)$  (for either  $i = 1$  or  $i = 2$ , the respective equations being identical), Eq. (2.6) takes the Schrödinger-like form

$$\phi'' - \frac{1}{u(1-u^2)^2} [K^2 - k^2 u^2 - u] \phi = 0, \quad (2.16)$$

where for the present purposes the potential can be approximated by

$$V = \frac{1}{u(1-u^2)^2} [K^2 - k^2 u^2]. \quad (2.17)$$

This potential is illustrated in Fig. 2b, for two values of the ratio  $k/K^3$ . As manifest in these figures, the potential barrier is now concentrated near the boundary at  $u = 0$ , within a distance  $u \lesssim 1/K^2$ , whereas the classically allowed region (i.e., the region where  $V(u) \leq 0$ ) starts at  $u = K/k$ . With increasing energy, the barrier does not disappear anymore, rather it gets squeezed towards  $u = 0$ , in such a way that its effects become smaller and smaller. At low energy, the wave can penetrate into the bulk only up to a small distance  $u \sim 1/K^2$  away from the boundary. But when the energy is so high that  $k/K^3 \sim \mathcal{O}(1)$ , the penetration distance  $\sim 1/K^2$  becomes of the same order as the classical turning point at  $K/k$ , and then the wave can freely escape in the allowed region at  $u > K/k$ , and thus get absorbed by the black hole.

These simple observations will be confirmed and substantiated by the subsequent analysis in this paper.

### 3. Low energy: the multiple scattering series

In this section we shall consider the low-energy regime at  $k/K^3 \ll 1$ , cf. Fig. 1a, where the effects of the term proportional to  $k^2$  in the potential  $V(u)$  (in either Eq. (2.15), or (2.17)) can be treated in perturbation theory. Note that, in terms of our original variables  $\omega$  and  $q$ , cf. Eq. (2.8), the condition  $k \ll K^3$  amounts to  $qT^2 \ll Q^3$ . Hence, for a fixed virtuality  $Q^2$ , the ‘low-energy’ regime can be also understood as a *low-temperature* one,  $T \ll (Q^3/q)^{1/2}$ , and the perturbative expansion that we shall shortly construct can be alternatively viewed as a multiple scattering series, or a low-temperature expansion.

Clearly, even when  $k \ll K^3$ , this perturbative expansion cannot work for arbitrary values of  $u$ : when  $u \gtrsim K/k$ , the energy-enhanced term  $\propto k^2$  in the potential becomes the *dominant* term there, which is responsible for the existence of the classically allowed region at  $u \geq K/k$ . Thus, not surprisingly, the perturbative treatment of the finite-energy/temperature effects cannot account for the contributions due to tunneling, which are genuinely non-perturbative and will be estimated in Appendix B within the WKB approximation. But if one leaves these contributions aside (they are exponentially suppressed anyway; see Appendix B), then perturbation theory should work reasonably well in the small- $u$  region at  $u \lesssim 1/K^2$ , which is the relevant region for computing the  $\mathcal{R}$ -current correlator, cf. Eqs. (2.11)–(2.12).

The main result that we shall arrive at in this section could be characterized as *negative*: we shall find that for  $k \ll K^3$  the DIS structure functions are strictly zero when computed to all orders in the multiple scattering (or ‘twist’) expansion. But the subsequent analysis is still interesting in that it provides the twist expansion for the real part of  $R_{\mu\nu}$ . In particular, from the leading term in this expansion (the single scattering approximation), we shall be able to deduce a couple of energy-momentum sum rules which will be very useful later on.

In the interesting region at  $u \lesssim 1/K^2 \ll 1$ , our key equations (2.6) and (2.9) simplify to

$$A_i'' - \frac{K^2}{u} A_i = -k^2 u A_i, \quad (3.1)$$

and, respectively,

$$a'' + \frac{1}{u} a' - \frac{K^2}{u} a = -k^2 u a. \quad (3.2)$$

In writing these equations, we have separated the terms  $\propto k^2$  in the r.h.s., anticipating that they are going to be treated as ‘small perturbations’. For consistency with the present approximations, which ignore the phenomenon of tunneling, the above equations must be solved with the condition that the fields vanish as  $u \rightarrow \infty$ . (This would be the correct boundary condition in the zero-temperature limit  $T \rightarrow 0$ , and it remains the appropriate boundary condition for a perturbative treatment of the finite-temperature effects.)

Consider first Eq. (3.2); after a change of variable  $\zeta \equiv 2K\sqrt{u}$ , this becomes

$$\left(\frac{d^2}{d\zeta^2} + \frac{1}{\zeta} \frac{d}{d\zeta} - 1\right) a(\zeta) = -\frac{k^2 \zeta^4}{16K^6} a(\zeta). \quad (3.3)$$

The zero-temperature limit<sup>2</sup> of this equation, that is,

$$\left(\frac{d^2}{d\zeta^2} + \frac{1}{\zeta} \frac{d}{d\zeta} - 1\right) a^{(0)}(\zeta) = 0, \quad (3.4)$$

describes the (longitudinal) metric perturbation induced by the  $\mathcal{R}$ -current in  $AdS_5$  in the absence of the black hole (the supergravity dual of an  $\mathcal{R}$ -current propagating through the gauge theory vacuum). The general solution to (3.4) is a linear combination of the modified Bessel functions  $K_0$  and  $I_0$ . The coefficient of  $I_0$  is set to zero by the condition of regularity as  $\zeta \rightarrow \infty$ , while that of  $K_0$  is fixed by the boundary condition at  $\zeta = 0$ , cf. Eq. (2.10). One thus finds

$$a^{(0)}(\zeta) = -2k^2 \mathcal{A}_L(0) K_0(\zeta). \quad (3.5)$$

The general equation (3.2) can be given a formal solution via Green’s function techniques :

$$a(\zeta) = a^{(0)}(\zeta) + \int_0^\infty d\zeta' G(\zeta, \zeta') \left(\frac{-k^2 \zeta'^4}{16K^6}\right) a(\zeta'), \quad (3.6)$$

with the Green’s function  $G(\zeta, \zeta')$  obeying

$$\left(\frac{d^2}{d\zeta^2} + \frac{1}{\zeta} \frac{d}{d\zeta} - 1\right) G(\zeta, \zeta') = \delta(\zeta - \zeta'), \quad (3.7)$$

together with the following boundary conditions

$$\begin{aligned} G(\zeta, \zeta') &\rightarrow 0 \quad \text{as } \zeta \rightarrow \infty, \\ \zeta \frac{d}{d\zeta} G(\zeta, \zeta') &\rightarrow 0 \quad \text{as } \zeta \rightarrow 0. \end{aligned} \quad (3.8)$$

It is easily checked that the corresponding solution reads

$$G(\zeta, \zeta') = -\zeta' \{K_0(\zeta) I_0(\zeta') \Theta(\zeta - \zeta') + K_0(\zeta') I_0(\zeta) \Theta(\zeta' - \zeta)\}. \quad (3.9)$$

The ‘solution’ (3.6) is truly an integral equation for  $a(\zeta)$ , which generates the multiple scattering series through iterations — here, for the longitudinal wave.

---

<sup>2</sup>The limit  $T \rightarrow 0$  of the present equations may look tricky since we have defined the dimensionless variables in Eq. (2.8) by dividing through  $T$ . However, in the zero-temperature case, one can view  $T$  in Eq. (2.8) as an arbitrary reference scale, introduced in order to define dimensionless variables. This scale cancels out in the final results for the current correlator at  $T = 0$ , as one can check on the examples of Eqs. (3.17) and (3.18) below.

Consider similarly the transverse sector. By replacing  $A_i = A_i(0)\zeta h(\zeta)$ , with  $\zeta = 2K\sqrt{u}$ , within Eq. (3.1), one finds

$$\left(\frac{d^2}{d\zeta^2} + \frac{1}{\zeta}\frac{d}{d\zeta} - 1 - \frac{1}{\zeta^2}\right)h = -\frac{k^2\zeta^4}{16K^6}h. \quad (3.10)$$

The zero-temperature version of this equation is solved by  $h^{(0)} = K_1(\zeta)$ , which obeys  $\zeta h^{(0)}(\zeta) \rightarrow 1$  as  $\zeta \rightarrow 0$ , as it should. (The other solution  $I_1(\zeta)$  is rejected by the condition of regularity at infinity.) The general equation (3.10) can then be rewritten as an integral equation similar to Eq. (3.6) with  $a^{(0)} \rightarrow h^{(0)}$  and the following Green's function

$$G(\zeta, \zeta') = -\zeta' \{K_1(\zeta)I_1(\zeta')\Theta(\zeta - \zeta') + I_1(\zeta)K_1(\zeta')\Theta(\zeta' - \zeta)\}. \quad (3.11)$$

As a simple application of the previous results, let us now compute the first two terms in the low-temperature expansion of the current-current correlator (2.1) — that is, its zero-temperature piece  $R_{\mu\nu}^{(0)}$ , which represents the vacuum polarization tensor of the  $\mathcal{R}$ -current, and the first temperature-dependent contribution  $R_{\mu\nu}^{(1)}$ , which describes the scattering between the  $\mathcal{R}$ -current and the  $\mathcal{N} = 4$  SYM plasma in the single-scattering, or ‘leading twist’, approximation. To that aim, we need the first two iterations in the above integral equations for  $a(u)$  and  $A_i(u)$ , evaluated near  $u = 0$  (cf. Eqs. (2.11)–(2.12)).

To the order of interest, we can write  $a(u) = a^{(0)}(u) + a^{(1)}(u)$ , where  $a^{(0)}(u)$  has a logarithmic singularity as  $u \rightarrow 0$ , as expected according to Eq. (2.10),

$$a^{(0)}(u) = k^2\mathcal{A}_L(0) (\ln K^2 + \ln u + 2\gamma + \mathcal{O}(u)) \quad (3.12)$$

( $\gamma = 0.577\dots$  is Euler's constant), while  $a^{(1)}(0)$  is finite and equal to

$$a^{(1)}(0) = \mathcal{A}_L(0) \frac{-2k^4}{16K^6} \int d\zeta \zeta^5 K_0^2(\zeta) = -\frac{2k^4}{15K^6} \mathcal{A}_L(0). \quad (3.13)$$

As for the transverse fields  $A_i(u)$ , these are needed up to linear order in  $u$ , i.e., to quadratic order in  $\zeta$ ; one finds  $A_i(u) = A_i^{(0)}(u) + A_i^{(1)}(u)$ , with

$$A_i^{(0)}(u) \simeq A_i(0) \left\{ 1 + uK^2 (\ln K^2 - 1 + \ln u + 2\gamma) \right\} \quad (3.14)$$

$$A_i^{(1)}(u) \simeq A_i(0) \frac{uk^2}{5K^4}. \quad (3.15)$$

When the  $T = 0$  fields in (3.12) and (3.14) are used to evaluate the vacuum action  $S^{(0)}$ , cf. Eq. (2.11), the result exhibits a logarithmic divergence coming from the limit  $u \rightarrow 0$ . As usual in the AdS/CFT context, this singularity is interpreted as a ultraviolet divergence in the dual gauge theory, to be removed via renormalization. To that aim, it is important to return to the original variables  $r$ ,  $\omega$ ,  $q$ , and  $Q^2 = q^2 - \omega^2$ , to make it clear that the UV ‘counterterms’ are indeed temperature-independent. Then, the relevant terms in the action are

$$\ln K^2 + \ln u = \ln \frac{Q^2}{4\pi^2 T^2} + \ln \frac{\pi^2 R^4 T^2}{r^2} = \ln \frac{Q^2}{\Lambda^2} + \ln \frac{R^4 \Lambda^2}{4r^2}, \quad (3.16)$$

where the  $T$ -dependence has disappeared, as anticipated, and  $\Lambda$  plays the role of the subtraction scale on the gauge theory side. For convenience, we renormalize by dropping the last term in the above equation together with the finite term  $2\gamma$ . We thus obtain  $S^{(0)} = \int d^4x \mathcal{S}^{(0)}$ , with

$$\mathcal{S}^{(0)} = -\frac{N^2}{64\pi^2} \ln \frac{Q^2}{\Lambda^2} [(qA_0 + \omega A_3)^2 - Q^2 \mathcal{A}_T \cdot \mathcal{A}_T]_{u=0}, \quad (3.17)$$

where we have introduced the transverse vector notation  $\mathcal{A}_T \equiv (A_1, A_2)$ . From this expression, one can immediately deduce the vacuum polarization tensor (with  $\eta_{\mu\nu} = (-1, 1, 1, 1)$ ) :

$$R_{\mu\nu}^{(0)}(q) = \left( \eta_{\mu\nu} - \frac{q_\mu q_\nu}{Q^2} \right) R_1^{(0)}(Q^2) \quad \text{with} \quad R_1^{(0)}(Q^2) = \frac{N^2 Q^2}{32\pi^2} \ln \frac{Q^2}{\Lambda^2}. \quad (3.18)$$

This is transverse, as required by current conservation, and moreover it has exactly the same expression as in zeroth-order (one loop) perturbation theory. This ‘non-renormalization’ property of the  $\mathcal{R}$ -current polarization tensor has been already observed in the literature, and proven to be a consequence of supersymmetry [65].

Similarly, by using the finite- $T$  contributions to the fields, Eqs. (3.13) and (3.15), one can compute the respective contribution to the on-shell action,  $S^{(1)} = \int d^4x \mathcal{S}^{(1)}$ , which is manifestly ultraviolet-finite :

$$\mathcal{S}^{(1)} = \frac{N^2 \pi^2 T^4}{30} \frac{q^2}{Q^6} \left[ (qA_0 + \omega A_3)^2 + \frac{3}{2} Q^2 \mathcal{A}_T^2 \right]_{u=0}, \quad (3.19)$$

From (3.19) one can determine the single-scattering, or low-temperature, part of the tensor  $R_{\mu\nu}$ . This has the structure exhibited in Eq. (A.1) with the following, ‘leading-twist’, expressions for the scalar components  $R_1$  and  $R_2$  :

$$R_1^{(1)} = \frac{N^2 \pi^2 T^2}{40x^2}, \quad R_2^{(1)} = \frac{N^2 \pi^2 T^4}{6Q^2}, \quad (3.20)$$

which are both *real* : as anticipated at the beginning of the section, the DIS structure functions vanish in the leading-twist approximation, and in fact to *all* orders in the twist expansion — indeed, all the terms generated by iterating the integral equation (3.6) for the longitudinal field, or the corresponding equation for the transverse fields, are obviously real.

Note the  $1/x^2$  behavior of  $R_1^{(1)}$ , which is the hallmark of the graviton exchange and reflects the fact that the contributions to  $R_{\mu\nu}$  computed in Eq. (3.20) come from the twist-two and spin-two operator  $T_{\mu\nu}$  (the energy-momentum tensor) in the operator product expansion (OPE) of the current-current correlator (2.1). This is the only leading-twist operator which survives in the OPE at strong coupling, since the other twist-two operators with spins  $j > 2$  acquire large anomalous dimensions  $\sim \lambda^{1/4} \rightarrow \infty$ . It is quite remarkable that the OPE coefficients of  $T_{\mu\nu}$  that we have (indirectly) computed at strong coupling are exactly the same as the corresponding coefficients at weak coupling, as we shall demonstrate via an explicit zeroth-order calculation in Appendix C. This non-renormalization is yet another manifestation of the high degree of symmetry of the  $\mathcal{N} = 4$  SYM theory (see also Ref. [68]).

Similarly, the multiple scattering series previously discussed can be interpreted as the exchange of arbitrarily many gravitons. One simple way of understanding the lack of an imaginary part in these multiple graviton exchanges is to note that the gravitons carry no four-dimensional

space–time momentum, as reflected in the fact that the metric only depends upon the radial variable  $u$  in  $AdS_5$ . Hence, because of energy–momentum conservation, the graviton exchanges cannot create on–shell final states, which would be the source for inelasticity.

We thus conclude that in the intermediate energy/low temperature regime at  $k \ll K^3$  (or, equivalently, at relatively large values  $x \gg T/Q$  for the Bjorken variable), the only non–trivial contributions to the DIS structure functions  $F_i \propto \text{Im } R_i$  arise via tunneling through the potential, and thus are necessarily small. In Appendix B, these contributions will be estimated in the WKB approximation as  $F_i \sim \exp\{-c(K^3/k)^{1/2}\}$ , where the prefactor  $c$  is a number of  $\mathcal{O}(1)$ . This estimate confirms that  $\text{Im } R_i$  remains extremely small so long as  $k \ll K^3$ . We thus draw the rather striking conclusion that the strongly–coupled plasma has essentially no point–like constituents at  $x$  larger than  $x_s \sim T/Q$ .

Finally, let us mention an interesting consequence of the leading–twist results in Eq. (3.20), which will be very useful in what follows. Introducing the variable  $z \equiv 1/x$  and assuming standard analytic properties for the current–current correlator in the complex  $z$  plane, one can relate the behaviour of  $R_i(z)$  near  $z = 0$ , where Eq. (3.20) applies, to the integral of the DIS structure function  $F_i \propto \text{Im } R_i$  along the cuts on the real axis in the physical region at  $|z| > 1$ . One thus obtain the following sum–rules (see Appendix A for details)

$$\mathcal{E} = 18T^2 \int_0^1 dx F_2(x, Q^2), \quad (3.21)$$

$$\mathcal{E} = 45T^2 \int_0^1 dx F_L(x, Q^2), \quad (3.22)$$

where  $F_1$  and  $F_2$  are defined in (A.2)–(A.3),  $F_L = F_2 - 2xF_1$  is the longitudinal structure function, and

$$\mathcal{E} = \frac{3\pi^2 N^2 T^4}{8} \quad (3.23)$$

is the energy density of the  $\mathcal{N} = 4$  SYM plasma in the strong coupling limit:  $\mathcal{E} = \Theta_{00}$ , with  $\Theta_{\mu\nu}$  the energy–momentum tensor of the plasma, cf. Eq. (A.4). The appearance of the energy density in the l.h.s.’s of equations (3.21) and (3.22) is in fact natural: as we shall further explain in Sect. 5, the integrals in their r.h.s.’s are proportional to the energy density carried by the plasma constituents, as probed in DIS with a resolution scale  $Q^2$ ; this should be the same as the total energy density in the plasma, and in particular be independent of  $Q^2$  — which is precisely the content of Eqs. (3.21)–(3.22).

But the previous results in this section also show that the relatively large values of  $x$ , such that  $x > T/Q$ , give only tiny contributions to the structure functions, which die away exponentially at large  $Q^2$  and hence cannot ensure the fulfillment of the sum–rules. Therefore, the only way for these sum–rules to be satisfied is that the integrals in their r.h.s.’s be saturated by contributions from ‘partons’ at smaller values of  $x \lesssim T/Q$ . This corresponds to the ‘high–energy’ situation in Fig. 1c, to the analysis of which we now turn.

#### 4. High energy: deep inelastic scattering

In this section, we shall consider the high–energy ( $k > K^3$ ), or small– $x$  ( $x < T/Q$ ), regime, which is the most interesting regime for our present analysis, since this is where the deeply

inelastic scattering truly occurs. In this regime, the potential barrier becomes ineffective — it has either completely disappeared (in the longitudinal sector, cf. Figs. 1c or 2a), or become so narrow that it gives no significant attenuation (in the transverse sector, cf. Fig. 2b) —, and then the gravitational waves induced by the  $\mathcal{R}$ -current can propagate towards large values of  $u \sim \mathcal{O}(1)$ , until they reach the black hole horizon at  $u = 1$  and thus get absorbed. As explained in Sect. 2, this absorption manifests itself via imaginary parts in the classical solutions, that we shall first compute, and from which we shall then deduce the DIS structure functions.

By lack of exact solutions to the wave equations (2.6) and (2.9), we shall consider approximations which are valid for very high energies, such that  $k \gg K^3$ , but which cannot capture the transition from quasi-elastic to deeply-inelastic scattering, which takes place around  $k \sim K^3$ . In Appendix D, we shall construct approximate solutions valid for generic values of  $u$ , by performing piecewise approximations (in particular, the WKB approximation) and then matching the intermediate solutions with each other. Here, however, we shall use a simpler strategy to calculate the classical action (2.11). To appreciate this strategy, let us first recall what was the main difficulty with this calculation: although the action involves the classical solution near  $u = 0$  alone, as manifest on Eq. (2.11), this solution is generally sensitive to the dynamics at large  $u \sim \mathcal{O}(1)$ , via the ‘outgoing wave’ boundary condition that one has to impose near the horizon. The important simplification that appears at high energy is that this boundary condition can now be imposed already at *relatively small* values  $u \ll 1$ , where the general equations reduce to simpler ones, that can be solved exactly. Indeed, in the absence of any potential barrier, there is no mechanism to generate reflected waves at intermediate values of  $u < 1$ ; hence, an incoming wave cannot be tolerated in the solution not even at  $u \ll 1$ , since it would necessarily describe reflection off the black hole. This argument will be confirmed by the more general construction in Appendix D, which will provide the same small- $u$  solutions as obtained below in this section.

Note an additional, important, simplification which occurs at high energy: when  $k \gg K^3$ , the term in the potential involving the virtuality  $K^2$  of the current becomes negligible as compared to the other terms there, for all the relevant values of  $u$  (for both longitudinal and transverse modes). This means, in particular, that our subsequent discussion also applies to a *time-like* ( $K^2 \equiv k^2 - \varpi^2 < 0$ ) current, provided its energy is high enough ( $k \gg |K|^3$ ).

Indeed, consider the longitudinal sector first. When increasing  $u$  from  $u = 0$ , the last term  $\propto k^2 u^2$  in the potential (2.15) becomes comparable to the first term  $\propto 1/4u$  already at the very small value  $u_0 = 1/(4k^2)^{1/3}$ , at which the term  $\propto K^2$  is still negligible. Hence, the latter is never relevant, as anticipated. In particular, for  $u \ll 1$ , the potential simplifies to

$$V \simeq -\frac{1}{u^2} \left[ \frac{1}{4} + k^2 u^3 \right] \quad \text{for} \quad u \ll 1, \quad (4.1)$$

which has a peak at  $u \sim u_0$ , cf. Fig.1c. By performing the corresponding approximations on Eq. (2.9), this equation becomes

$$a'' + \frac{1}{u} a' + k^2 u a = 0, \quad (4.2)$$

which can be easily solved: after changing variable according to  $\xi \equiv \frac{2}{3} k u^{3/2}$ , we obtain

$$\left( \frac{d^2}{d\xi^2} + \frac{1}{\xi} \frac{d}{d\xi} + 1 \right) a(\xi) = 0 \quad (4.3)$$

which has the general solution

$$a(\xi) = c_1 J_0(\xi) + c_2 N_0(\xi), \quad (4.4)$$

where  $J_0$  and  $N_0$  are the usual Bessel and Neumann functions. Recalling the behaviour of these functions near  $\xi = 0$ , one sees that the boundary condition (2.10) fixes the coefficient  $c_2$ ,

$$c_2 = \frac{\pi k^2}{3} \mathcal{A}_L(0), \quad (4.5)$$

but has no consequence for  $c_1$ . To also determine the latter, we shall impose, as announced, the outgoing-wave boundary condition at sufficiently large values of  $u$ . Note that, although  $u$  is small,  $u \ll 1$ , the argument  $\xi$  of the Bessel functions becomes large,  $\xi \gg 1$ , for all the values of  $u$  far beyond the peak of the potential:  $u \gg u_0 \sim 1/k^{2/3}$ . In that region, one can use the asymptotic expressions for the Bessel functions, that is,  $J_0(\xi) \simeq \sqrt{2/\pi\xi} \cos(\xi - \pi/4)$  and  $N_0(\xi) \simeq \sqrt{2/\pi\xi} \sin(\xi - \pi/4)$ . If one also remembers the exponential factor yielding the time-dependence, cf. Eq. (2.4), it becomes clear that a purely outgoing-wave solution  $a(t, \xi) \propto e^{-i(\omega t - \xi)}$  is obtained by choosing

$$c_1 = -ic_2. \quad (4.6)$$

One thus obtains the following expression for the longitudinal solution in the region  $u \ll 1$

$$a(u) \simeq -i \frac{\pi k^2}{3} \mathcal{A}_L(0) H_0^{(1)} \left( \frac{2}{3} k u^{3/2} \right) \quad \text{for} \quad u \ll 1, \quad (4.7)$$

where  $H_0^{(1)} = J_0 + iN_0$  is a Hankel function.

A similar discussion applies to the transverse waves, which satisfy Eq. (2.6), or (2.16). In the high-energy regime at  $k \gg K^3$ , one can neglect the effects of the extremely narrow potential barrier located at  $0 < u < K/k$ . Indeed, the width  $K/k$  of the barrier is much smaller than the distance  $\sim 1/K^2$  over which the solution near  $u = 0$  would start to significantly differ from its boundary value at  $u = 0$ . In the small- $u$  region at  $K/k \lesssim u \ll 1$ , the potential (2.17) reduces to  $V \simeq -k^2 u$  and then both Eq. (2.6) and Eq. (2.16) reduce to

$$A_i'' + k^2 u A_i = 0. \quad (4.8)$$

This is an Airy equation whose general solution can be written as a linear combination of  $\text{Ai}(-uk^{2/3})$  and  $\text{Bi}(-uk^{2/3})$  or, equivalently [66], in terms of the Bessel functions of argument  $\nu = 1/3$ . We choose this latter representation, for more symmetry with the previous discussion; we thus write (with  $\xi = \frac{2}{3} u^{3/2} k$ , as before)

$$A_i(\xi) = \xi^{1/3} [c_1 J_{1/3}(\xi) + c_2 N_{1/3}(\xi)], \quad (4.9)$$

where  $c_2$  is determined from the value of  $A_i$  at  $u = 0$  and we again choose  $c_1 = -ic_2$ , in order for the solution to become a purely outgoing wave when  $u \gg 1/k^{2/3}$ . One finally gets the following result at small  $u$ :

$$A_i(u) \simeq A_i(0) \frac{i\pi}{\Gamma(1/3)} \left( \frac{k}{3} \right)^{1/3} \sqrt{u} H_{1/3}^{(1)} \left( \frac{2}{3} k u^{3/2} \right) \quad \text{for} \quad u \ll 1, \quad (4.10)$$

which now features the Hankel function  $H_{1/3}^{(1)} = J_{1/3} + iN_{1/3}$ .

By putting together the previous results (4.7) and (4.10), one can evaluate the on-shell action according to (2.11); this gives  $S = \int d^4x \mathcal{S}$  with

$$\mathcal{S} = -\frac{N^2 T^2}{48} \left[ k^2 \mathcal{A}_L^2(0) \left( 2\left(\gamma + \ln \frac{k}{3}\right) - i\pi \right) + \frac{9\pi}{\Gamma^2(1/3)} \left(\frac{k}{3}\right)^{2/3} \left(\frac{1}{\sqrt{3}} - i\right) \mathcal{A}_T^2(0) \right]. \quad (4.11)$$

Note the emergence of the imaginary part in the action (4.11), which has the right sign ( $\text{Im } \mathcal{S} > 0$ ) to describe dissipation, i.e., to yield positive contributions to the DIS structure functions. A simple calculation using Eqs. (2.12), (A.1), (A.2) and (A.3), finally leads to the following expressions for the structure functions at small  $x \ll x_s \sim T/Q$ :

$$F_1 = \frac{3N^2 T^2}{16\Gamma^2(1/3)} \left(\frac{k}{3}\right)^{2/3}, \quad (4.12)$$

$$F_L \equiv F_2 - 2xF_1 = \frac{N^2 Q^2 x}{96\pi^2}, \quad (4.13)$$

which represent our main result in this paper. Although strictly valid only for  $x \ll x_s$ , these results remain parametrically correct also in the transition region at  $x \simeq x_s$ . For  $x \gg x_s$ , on the other hand, the structure functions are negligibly small, as discussed in Sect. 3.

To render the above results more transparent, it is convenient to rewrite them in terms of the conventional variables for DIS,  $x$  and  $Q^2$ , and to also introduce the transverse structure function  $F_T \equiv 2xF_1$ , such that  $F_2 = F_T + F_L$ . Then Eqs. (4.12) and (4.13) imply the following parametric estimates:

$$\begin{aligned} F_T(x, Q^2) &\sim N^2 \frac{T^2}{x} \left(\frac{x^2 Q^2}{T^2}\right)^{2/3}, \\ F_L(x, Q^2) &\sim N^2 \frac{T^2}{x} \left(\frac{x^2 Q^2}{T^2}\right), \end{aligned} \quad (4.14)$$

which show that, in the very small- $x$  regime at  $x \ll T/Q$ , the longitudinal structure function is negligible as compared to the transverse one,  $F_L \ll F_T$ , and thus, somehow surprisingly, an analog of the Callan–Gross relation applies:  $F_2 \simeq 2xF_1$ . This looks surprising since it is quite different from what happens in the case where the target is a single hadron, at either weak coupling<sup>3</sup> [59], or strong coupling [57, 58], where in the high-energy limit  $F_L$  and  $F_T$  are parametrically of the same order.

## 5. Saturation and the partonic structure of the plasma

The results of the last two sections are conveniently described using Fig. 3 where  $\tau \equiv \ln 1/x$  is the ‘rapidity’ and  $\rho \equiv \ln(Q^2/T^2)$ . For a given  $\rho \gg 1$  and values of  $\tau$  below the *saturation line*

---

<sup>3</sup>In QCD at weak coupling, the Callan–Gross relation holds only in the Bjorken scaling regime at relatively large  $x$ , where the structure functions are dominated by the valence quarks and depend very weakly upon  $Q^2$ .

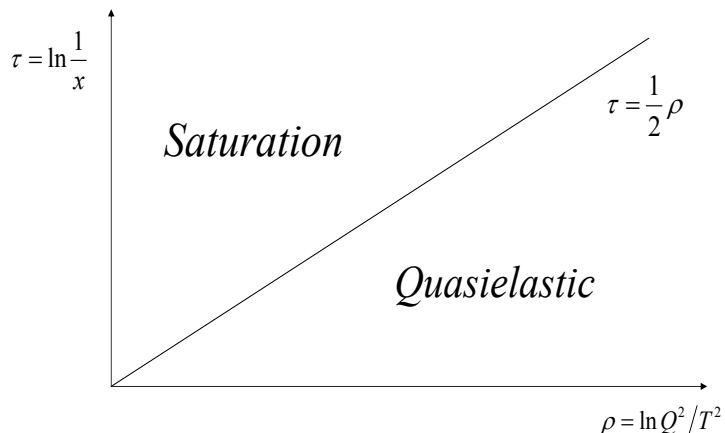


**Figure 3:** Proposed ‘phase diagram’ for DIS off a  $\mathcal{N} = 4$  SYM plasma at high energy and strong coupling.

$\tau_s(\rho) = \rho/2$ , meaning  $x \gg x_s \simeq T/Q$ , the structure functions are *extremely* small (cf. Eq. (B.10) in Appendix B),

$$F_{L,T} \sim N^2 Q^2 x \exp\{-c(x/x_s)^{1/2}\} \propto \exp\{-c e^{(\tau_s - \tau)/2}\} \quad \text{for} \quad \tau < \tau_s(\rho), \quad (5.1)$$

while for values of  $\tau$  significantly above that line ( $x \ll x_s$ ) the structure functions take on the values given in (4.12) and (4.13). The transition between these two regimes when crossing the saturation line is expected to occur within a rapidity interval  $\Delta\tau \sim \mathcal{O}(1)$ .

The saturation line can equivalently be rewritten as  $\rho_s(\tau) = 2\tau$ , and then the estimates (5.1) for the structure functions at small  $\tau$  are tantamount to

$$F_i \sim \exp\{-c(Q/Q_s)^{1/2}\} \sim \exp\{-c e^{(\rho - \rho_s)/2}\} \quad \text{for} \quad \rho > \rho_s(\tau), \quad (5.2)$$

with the *saturation momentum*

$$Q_s^2(\tau) \equiv T^2 e^{\rho_s} = T^2 e^{2\tau} = \frac{T^2}{x^2}. \quad (5.3)$$

Such a small value for  $F_i$  for large  $Q^2 \gg Q_s^2(\tau)$  is qualitatively consistent with previous calculations of the dilaton structure functions at strong coupling [57, 58], although some quantitative differences remain. In these previous works, one has found that the higher-twist terms dominate the dilaton structure functions at large  $Q^2$ , thus yielding a fast decrease with  $Q^2$ , which is however *power-like*,  $F_i(x, Q^2) \propto (1/Q^2)^\Delta$  with  $\Delta \geq 1$ , rather than exponential as predicted by Eq. (5.2). Some of these higher-twist contributions are naturally absent from the present analysis, since suppressed in the large- $N$  limit. (This is the case for the diffractive processes considered in Ref. [58], which in the present framework would correspond to multiple scattering

off a *same* thermal quasiparticle. The corresponding scattering amplitude starts at order  $1/N^4$ , and hence it is suppressed at large  $N$  even after multiplication by the number  $\sim N^2$  of thermal degrees of freedom.) On the other hand, the higher-twist contributions due to protected operators, as discussed for a dilaton target in Ref. [57], would survive in large- $N$  limit, but they are removed by the requirement of energy-momentum conservation. (Being homogeneous in the four physical dimensions, the plasma cannot transmit any energy or momentum via a single scattering.) We interpret this smallness of  $F_i$  at relatively large  $x$  to mean that for  $x \gg x_s = T/Q$  there are hardly any point-like excitations (partons) in the SYM plasma.

In what follows, we shall rather focus on the more interesting situation at  $x \lesssim x_s$ , or large rapidity  $\tau \gtrsim \tau_s(\rho)$ , where partons *do* exist, as we shall see. A natural place to look for a partonic interpretation is at the level of the sum rules (3.21) and (3.22). By inspection of our previous estimates (4.14) for the structure functions, it is easy to check that (i) the integrals in Eqs. (3.21) and (3.22) are dominated by values of  $x$  of order  $x_s$  (for which the transverse and longitudinal structure functions are of the same order of magnitude), and (ii) the results of these integrations are of the right order of magnitude, namely of  $\mathcal{O}(N^2 T^4)$ , to ensure the fulfillment of the sum rules. For instance, for Eq. (3.21) we can write

$$\mathcal{E} = 18T^2 \int_0^1 dx F_2(x, Q^2) \sim T^2 x F_2(x, Q^2) \Big|_{x=T/Q}, \quad (5.4)$$

where  $x F_2(x, Q^2) \sim N^2 T^2$  when  $x \simeq T/Q$ , as manifest from Eq. (4.14) (recall that  $F_2 = F_T + F_L$ ). Ours results in Eqs. (4.12)–(4.13) are not accurate enough to also check the numerical coefficients in front of the sum rules (this would require a more precise study of the transition region at  $x \sim x_s$ ). But the parametric estimates in Eq. (4.14) are sufficient for our present purpose, which is to develop a partonic picture for the strongly coupled plasma.

Before we proceed, let us first recall the interpretation of the structure function  $F_2$  in the more familiar context of perturbative QCD. In that case,  $F_2(x, Q^2)$  is a dimensionless quantity interpreted as the *quark distribution* in the proton target, i.e., the number of quarks which are localized in impact parameter space within an area  $\sim 1/Q^2$  fixed by the resolution of the virtual photon, and which are distributed in longitudinal phase-space within a unit of rapidity ( $\Delta\tau \sim 1$ ) around the rapidity  $\tau = \ln(1/x)$  fixed by the Bjorken variable. In what follows, we shall boldly propose a similar interpretation for the strongly-coupled plasma, and then critically examine the most sensible points in our proposal.

Unlike the proton, or dilaton, structure functions, which are dimensionless, the plasma structure functions  $F_i$  as computed in this paper have dimensions of  $(\text{area})^{-1}$ . This makes it natural to try and relate these functions to the density of partons per unit area in the transverse plane  $(x, y)$  (the impact parameter space). The  $\mathcal{R}$ -current with  $Q^2 \gg T^2$  probes an area  $\sim 1/Q^2$  much smaller than the typical area  $\sim 1/T^2$  covered by a ‘thermal quasiparticle’ in the plasma — i.e., a typical thermal excitation with energy and momentum of order  $T$  (in the plasma rest frame). This means that the current can see ‘inside’ a quasiparticle, and thus probe its elementary constituents, or ‘partons’. More precisely, it will simultaneously scrutinize inside all the quasiparticles located within one *coherence length* in the longitudinal direction  $z$ . The notion of coherence length is particularly important for what follows, and so is also the choice of an appropriate Lorentz frame in which the parton interpretation makes sense. So, let us open a parenthesis at this point, in order to better explain these concepts :

(i) The partonic picture makes sense in a frame where the current has low energy and a relatively simple internal structure, so that it can act as a probe of the target. Here, it will be convenient to use the Breit frame where the  $\mathcal{R}$ -current is a standing wave. Namely, if one boosts the plasma by an amount  $\eta$  where  $\cosh \eta = q/Q$ , then in this boosted frame the current has time and  $z$ -momentum components  $\omega' = 0$  and  $q' = Q$ . This current is naturally absorbed by partonic constituents of the boosted plasma having momenta of order  $Q$ . Indeed, the partons participating in the collision have a longitudinal momentum fraction  $x$ , and thus a typical momentum  $p'_z \sim x(T \cosh \eta) \sim Q$  in the boosted frame.

(ii) Before boosting, the current correlator (2.1) is sensitive to longitudinal distances  $\Delta z \lesssim 2q/Q^2$ , as is suggested by writing the space-time dependence in the integral there as

$$e^{-i\omega t + iqz} \simeq e^{-iq(t-z) + iQ^2 t/2q}, \quad (5.5)$$

where we have used  $Q^2 \simeq 2q(q - \omega)$  for  $q^2 \gg Q^2$ . This shows that the integration in (2.1) can extend over the coherence time  $\Delta t_c \sim 2q/Q^2$ , corresponding to a coherence length  $\Delta z_c \sim 2q/Q^2$  in the plasma rest frame. After the boost, this length gets Lorentz contracted (note that the current is decelerated) down to a value  $\Delta z'_c \sim (2q/Q^2)/\cosh \eta \sim 1/Q$ .

Let us now return to Eq. (5.4) and try to interpret this sum rule in the Breit frame. In the l.h.s., we would like to construct the energy density per unit area,  $dE'/d^2b$ , of the region of the plasma which is explored by the  $\mathcal{R}$ -current in this boosted frame. As a component of the second-rank tensor  $\Theta_{\mu\nu}$ , the (three-dimensional) energy density  $\mathcal{E}$  transforms in the boost by a factor  $(\cosh \eta)^2$ . The  $\mathcal{R}$ -current probes a slice of the plasma with longitudinal extent  $\Delta z'_c$  in the boosted frame. Hence,  $dE'/d^2b \sim (\mathcal{E} \cosh^2 \eta) \Delta z'_c \simeq \mathcal{E}(2q/Q^2) \cosh \eta$ . Multiplying both sides of (5.4) by  $(2q/Q^2) \cosh \eta$ , one gets

$$\frac{dE'}{d^2b} \sim xT \cosh \eta \left( \frac{1}{x} F_2(x, Q^2) \right)_{x=T/Q}. \quad (5.6)$$

As before mentioned, the quantity  $xT \cosh \eta \sim Q$  in the r.h.s. is the longitudinal momentum of the constituent (parton) which interacts with the  $\mathcal{R}$ -current. It is therefore natural to interpret

$$\frac{1}{x} F_2(x, Q^2) \Big|_{x=T/Q} \sim \frac{dn}{d^2b} \Big|_{x=T/Q}, \quad (5.7)$$

as the number of partons per unit area within a longitudinal slice of the plasma, with the width of the slice equal to the coherence length (which is  $1/Q$  in the Breit frame, and  $q/Q^2$  in the plasma rest frame). This interpretation, which here has been inferred from the sum rule (5.4), is in fact natural in view of the standard partonic interpretation of  $F_2$  at weak coupling, as alluded to before. The only new feature with respect to the case where the target is a single proton<sup>4</sup> is the factor  $1/x$  in the l.h.s.: this is a Lorentz-invariant measure of the amount of matter in the plasma in the longitudinal slice explored by the current. Namely, this has been generated as (say, in the plasma rest frame):  $T \Delta z_c \sim 1/x$ , where  $T$  is the density of quasi-particles per unit length and  $\Delta z_c$  is the longitudinal extent of the interaction region.

---

<sup>4</sup>There is no such a factor in the case of a single-hadron target since there the whole longitudinal extent of the hadron lies within one coherence length for the virtual photon.

For what follows, it is useful to notice that the parton density in the r.h.s. can be equivalently written

$$\frac{dn}{d^2b} = \Delta z' \frac{dn}{dz'd^2b} \simeq \frac{dn}{p'_z dz' d^2b} = \frac{dn}{d\tau d^2b}, \quad (5.8)$$

where  $\Delta z' \sim 1/Q$  is the longitudinal extent of the slice in the boosted frame and  $p'_z \sim Q$  (the  $z$ -momentum of a struck parton) is the same as  $1/\Delta z'$ , as it should by the uncertainty principle. In writing the last equality, we have identified the rapidity interval  $d\tau = p'_z dz'$ .

By using Eq. (5.7) together with the previous estimate (4.14) for  $F_2 = F_T + F_L$ , one finds

$$\frac{dn}{d\tau d^2b} \sim N^2 Q^2 \quad \text{for} \quad x \sim T/Q, \quad (5.9)$$

which, remarkably, has the same parametric form as in a weakly-coupled gauge theory [59], and hence it admits a similar physical interpretation. Namely, when interpreted in the Breit frame, Eq. (5.9) gives the total number of partons (per unit area) having a longitudinal momentum fraction equal to  $x$  (with  $x \lesssim T/Q$ ) and with transverse momenta  $p_\perp \lesssim Q$ . Since this number appears to be of order  $N^2 Q^2$ , we conclude that there is a number of order one of partons (of a given color) per unit of phase-space:

$$\frac{1}{N^2} \frac{dn}{d\tau d^2p_\perp d^2b_\perp} \simeq 1 \quad \text{for} \quad p_\perp \lesssim Q_s(x) = T/x. \quad (5.10)$$

(The factor  $d\tau$  plays the role of  $p'_z dz'$ , cf. Eq. (5.8), so the above phase-space density is an *occupation number*, in the proper, three-dimensional, sense.) This is similar to pQCD in the sense that the parton occupation number saturates at sufficiently low transverse momenta, below a critical scale  $Q_s(x)$  which grows like a power of  $1/x$ . In QCD, saturation is a reflection of unitarity in a corresponding scattering process. Where is the unitarity limit here? Viewed on the gravity side of the AdS/CFT correspondence the gravitational wave  $A_\mu$  induced by the  $\mathcal{R}$ -current is completely absorbed at the horizon of the black hole and that absorption takes place over a time less than or equal to the coherence time,  $1/xT$ , of the wave. This is, in effect, a unitarity limit for scattering of the gravitational wave (very much similar to the corresponding limit for dipole scattering in the familiar dipole factorization for DIS at high energy [59]).

Recently, the phenomenon of parton saturation in relation with the unitarity limit for DIS has also been identified at *strong coupling*, in the case where the target is a single ‘hadron’ (a dilaton) [58]. Interestingly, our above result (5.3) for the saturation momentum of the plasma is consistent with the corresponding result for a single hadron in Ref. [58], once the assumed structure of the SYM plasma in terms of quasiparticles is taken into account. Namely, the quantity  $Q_s^2$  is proportional to the density of partons per unit area in impact parameter space. In the case of a single dilaton, Ref. [58] has found

$$Q_s^2(x) = \frac{\Lambda^2}{xN^2} \quad (\text{one dilaton target}), \quad (5.11)$$

with  $1/\Lambda$  a measure of the dilaton transverse size. When moving to the plasma, the dilaton gets replaced by thermal quasiparticles with individual size  $\sim 1/T$ . To account for the degrees of freedom relevant to DIS, one must sum over color (this yields a factor  $N^2$ ) and also over the

number of quasiparticles within a longitudinal slice of width  $\Delta z_c \sim q/Q^2$  in the plasma rest frame (which gives an additional factor  $T\Delta z_c \sim 1/x$ ). After replacing  $\Lambda \rightarrow T$  in Eq. (5.11) and putting these various factors together, we end up with the previous result, Eq. (5.3), as anticipated. This is an important check of the internal consistency of our proposed partonic description — it comforts our idea that DIS off the plasma at high  $Q^2 \gg T^2$  should measure the internal constituents of the thermal quasiparticles composing the plasma. This check is particularly non-trivial in view of the fact that the unitarization mechanisms at work appear to be very different in the two cases — disappearance of the potential barrier for the plasma case, respectively, diffractive scattering via multiple graviton exchanges in the dilaton case.

We now turn to the case  $x \ll T/Q$ , which turns out to be quite subtle. Previously, we argued that the typical interaction time is of the order of the coherence time  $\Delta t_c \sim q/Q^2$  of the incoming current. This argument, however, ceases to be valid at very high energy, where the gravitational wave gets absorbed (reaches the horizon) on a time scale shorter than  $\Delta t_c$ . A heuristic way to understand this is to recall that, when the energy is so high that the barrier has disappeared, cf. Fig. 1c (namely, for  $qT^2/Q^3 \gg 1$ ), the  $F_1$  structure function becomes independent of  $Q^2$ , as manifest on Eq. (4.12). On the other hand, the definition (2.1) of the current-current correlator involves an explicit dependence upon  $Q^2$ , via the exponential factor inside the integrand, conveniently written as in Eq. (5.5). The only way for this dependence to disappear at high energy is that the integral over  $t$  in Eq. (2.1) be cut at some time which is considerably shorter than the coherence time  $\Delta t_c$ . This requires the lifetime of the gravitational wave (before being absorbed by the black hole) to be shorter than  $\Delta t_c$ . For a given energy  $q$ , this lifetime can be estimated as  $q/Q_s^2(q)$ , since  $Q^2 = Q_s^2(q)$  is the smallest value of  $Q$  for which Eqs. (2.9) and (2.6) still have a  $Q$ -dependence. Here,  $Q_s^2(q)$  is the saturation momentum expressed as a function of  $q$ , and is obtained from the condition  $qT/Q_s^2 = Q_s/T$  (the condition to lie on the saturation line in Fig. 3) as  $Q_s^2(q) = (qT^2)^{2/3}$ . Note that  $q/Q_s^2(q)$  is indeed much smaller than  $q/Q^2$  in this high energy regime.

Because of this short lifetime of the high-energy gravitational wave, we believe that the quantity  $F_1(x, Q^2) \simeq (1/2x)F_2(x, Q^2)$  (which, we recall, is the dominant structure function when  $x \ll T/Q$ ) is actually being determined by interactions of the  $\mathcal{R}$ -current with partons of size  $1/Q_s^2(q)$ , rather than with partons of size  $1/Q^2$ . Indeed, Eq. (4.12) implies

$$F_1(x, Q^2) = F_1(x_s, Q_s^2) \quad \text{where} \quad Q_s^2(q) = (qT^2)^{2/3} \quad \text{and} \quad x_s(q) = T/Q_s(q). \quad (5.12)$$

Let us give another argument leading to the same conclusion. We recall that in DIS in the QCD dipole picture, and in the rest frame of the target, the size of the dipole emerging from the electromagnetic current expands with time as  $\Delta x_\perp \sim \sqrt{t/2q}$  [70], so that it takes a time  $t \sim 2q/Q^2$  for this dipole to reach a size  $\Delta x_\perp \sim 1/Q$ . Assume that a similar estimate applies for the SYM system emerging from the  $\mathcal{R}$ -current (the analog of the QCD color dipole); then, after a time  $t_s \sim 2q/Q_s^2(q)$ , which is the lifetime of this SYM system before being absorbed by the plasma, its size gets only as big as  $\Delta x_\perp \sim 1/Q_s(q)$ , which indicates once again that the partons at scale  $Q_s(q)$  are the relevant degrees of freedom.

We shall conclude this discussion, and also the paper, with a critical analysis of the main assumptions that we have made in reaching Eqs. (5.7) and (5.9) — the equations at the basis of our partonic interpretation. (i) We have assumed the plasma to be made of constituents

(‘quasiparticles’) having momenta on the order of  $T$  (in the plasma rest system) when measured on a resolution scale  $T$ . The fact that entropy density and energy density scale as  $N^2T^3$  and  $N^2T^4$  suggest that this is the case, but this understanding is, perhaps, not completely clear. Note that, for the present purposes, we did not need to specify the actual nature of these ‘quasiparticles’, which at strong coupling would be a most difficult task. (ii) We have also assumed that the  $\mathcal{R}$ -current directly measures individual constituents at scale  $Q$ . In QCD the electromagnetic current provides such a measurement in the leading order renormalization group formalism. At next-to-leading order, ambiguities occur in separating the measured partons from the probe; however, these ambiguities are effects of order  $\alpha(Q^2)$  and cannot affect general conclusions as to numbers of partons in a hadron or plasma. In SYM, we have taken the coupling large so that the separation between the probe and the partons to be measured is not sharp anymore. In reaching (5.7) and (5.9) we have assumed that, up to factors of order one, the  $\mathcal{R}$ -current couples to individual constituents of the plasma and that this coupling is not strongly renormalized. Because of these subtleties we feel that our results have to be taken with caution, and that a deeper understanding of the partonic structure of the plasma in strong coupling SYM is highly desirable.

## Acknowledgments

We would like to thank Iosif Bena for useful discussions. The work of A.H. M. is supported in part by the US Department of Energy. The work of E. I. is supported in part by Agence Nationale de la Recherche via the programme ANR-06-BLAN-0285-01.

## A. Structure functions: Definitions and sum rules

In this appendix we remind the reader of the tensor structure of  $R_{\mu\nu}$  and derive a sum rule relating the expectation of energy momentum tensors in the plasma to deep inelastic scattering on the plasma.  $R_{\mu\nu}$  is defined in Eq. (2.1), The tensor structure must be given in terms of  $q^\mu$  and the plasma four-velocity  $n^\mu = (n_t, n_x, n_y, n_z)$ , with  $n^\mu = (1, 0, 0, 0)$  corresponding to the plasma at rest. Then current conservation plus the symmetry property  $R_{\mu\nu}(q) = R_{\nu\mu}(-q)$  imply the following general structure (with  $\eta_{\mu\nu} = (-1, 1, 1, 1)$ ) :

$$R_{\mu\nu} = \left( \eta_{\mu\nu} - \frac{q_\mu q_\nu}{Q^2} \right) R_1 + \left[ n_\mu n_\nu - \frac{n \cdot q}{Q^2} (n_\mu q_\nu + n_\nu q_\mu) + \frac{q_\mu q_\nu}{(Q^2)^2} (n \cdot q)^2 \right] R_2. \quad (\text{A.1})$$

The two scalar functions  $R_1$  and  $R_2$  depend upon the two invariants  $Q^2$  and  $x$  introduced in Eq. (2.13), and they are even functions of  $x$ . We define the DIS structure functions as (note that  $n \cdot q = -\omega$  is negative)

$$F_1 = \frac{1}{2\pi} \text{Im}R_1, \quad (\text{A.2})$$

$$F_2 = \frac{-(n \cdot q)}{2\pi T} \text{Im}R_2. \quad (\text{A.3})$$

Writing the energy-momentum tensor of the plasma as

$$\Theta_{\mu\nu} = (\eta_{\mu\nu} + 4n_\mu n_\nu) \frac{\mathcal{E}}{3} \quad \text{with} \quad \mathcal{E} = \frac{3N^2\pi^2 T^4}{8}, \quad (\text{A.4})$$

we can rewrite the leading-twist results in Eq. (3.20) as

$$R_1^{(1)} = \frac{\mathcal{E}}{15T^2 x^2}, \quad R_2^{(1)} = \frac{4\mathcal{E}}{9Q^2}. \quad (\text{A.5})$$

This rewriting makes it clear that the calculation of the leading-twist contribution to  $R_{\mu\nu}$  in Sect. 3 amounts to computing the coefficients of the energy-momentum tensor in the operator product expansion for the current-current correlator.

To deduce the sum rules (3.21) and (3.22), we shall write  $z = 1/x$  and assume the standard analytic structure for the functions  $R_i(z)$  in the complex  $z$  plane. Namely,  $R_i(z)$  is an analytic function everywhere in the complex plane except for two cuts along the real axis (from  $z = -\infty$  to  $z = -1$  and, respectively, from  $z = 1$  to  $z = \infty$ ). Then our previous results in Eq. (A.5) express the dominant behaviour of  $R_i(z)$  near  $z = 0$ . Using this information together with Eq. (A.5), we can successively write

$$\begin{aligned} \frac{4\mathcal{E}}{9Q^2} &= \oint \frac{dz}{2\pi i} \frac{R_2}{z} = 2 \int_1^\infty \frac{dz}{2\pi i} \frac{2i \operatorname{Im} R_2}{z} \\ &= \frac{2}{\pi} \int_0^1 dx \frac{\operatorname{Im} R_2}{x} = \frac{8T^2}{Q^2} \int_0^1 dx F_2(x, Q^2) \end{aligned} \quad (\text{A.6})$$

where the contour in the first integral is a small circle surrounding the origin. This is then distorted in the complex plane in such a way to wrap around the two branch cuts which give equal contributions. (We assume the integrand to vanish sufficiently fast as  $|z| \rightarrow \infty$  to be able to neglect the contributions of the large circles closing the contour.) Similarly,

$$\begin{aligned} \frac{\mathcal{E}}{15T^2} &= \oint \frac{dz}{2\pi i} \frac{R_1}{z^3} = 2 \int_1^\infty \frac{dz}{2\pi i} \frac{2i \operatorname{Im} R_1}{z^3} \\ &= \frac{2}{\pi} \int_0^1 dx x \operatorname{Im} R_1 = 4 \int_0^1 dx x F_1(x, Q^2) \end{aligned} \quad (\text{A.7})$$

## B. Low energy: tunnel effect

In this Appendix we shall use WKB techniques to estimate the probability for inelastic scattering via tunnel effect in the intermediate energy regime at  $Q \ll q \ll Q^3/T^2$ , where the potential barrier is high. The argument turns out to be non-trivial because the imaginary part of the classical solution — which, we recall, is the measure of inelasticity in the scattering — gets built via a ‘double-tunnel effect’ (see below), for which the WKB approximation is generally not reliable. Yet, as we shall later argue, in the present setup this approximation should be reliable for the imaginary part of the solution.

We shall focus on the longitudinal wave (the corresponding discussion of the transverse wave is entirely similar) and use the wave equation in Schrödinger form, cf. Eqs. (2.14)–(2.15). We shall construct our global approximation for  $\psi$  by matching approximate solutions valid in three different domains: (i)  $u$  close to zero, (ii)  $u$  inside the potential barrier in Fig. 1a, and (iii) relatively large  $u$ , on the right side of the barrier. As usual, the imaginary part in the solution will be generated by the condition that  $\psi(u)$  be a purely outgoing wave at large  $u \sim \mathcal{O}(1)$ .

(i) For relatively small  $u$ , the potential in Eq. (2.15) can be approximated as

$$V \simeq \frac{1}{u} \left[ -\frac{1}{4u} + K^2 \right] \quad \text{for} \quad 0 \leq u \ll K/k. \quad (\text{B.1})$$

Then the general solution can be written as:

$$\psi(u) = C_1 \sqrt{u} K_0(2K\sqrt{u}) + C_2 \sqrt{u} I_0(2K\sqrt{u}), \quad (\text{B.2})$$

where the coefficient  $C_1$  is fixed by the boundary condition at  $u = 0$ , Eq. (2.10), as  $C_1 = -2k^2 \mathcal{A}_L(0)$ . This approximation is similar to the zeroth order perturbative solution (3.5) in Sect. 3 except that, now, the coefficient  $C_2$  in front of  $I_0$  is allowed to be non-zero because of the different behaviour assumed at large  $u$ . The imaginary part,  $\text{Im } C_2$ , of this coefficient is the quantity that we are primarily interested in, because this quantity determines, via Eq. (2.11), the imaginary part of the ‘on-shell’ action.

(ii) For values of  $u$  inside the potential barrier,  $u_1 < u < u_2$  with  $u_1 \simeq 1/(4K^2)$  and  $u_2 \simeq K/k$  the two classical turning points in Fig. 1a, the solution can be constructed via the WKB approximation, which yields

$$\psi(u) \simeq \frac{1}{\sqrt{V(u)}} \left[ C_3 \exp \left\{ - \int_{u_1}^u du' \sqrt{V(u')} \right\} + C_4 \exp \left\{ \int_{u_1}^u du' \sqrt{V(u')} \right\} \right]. \quad (\text{B.3})$$

In applications of the WKB technique to the tunnel effect, the analog of the second term in the equation above is generally omitted, since beyond the accuracy of this approximation. However, in so far as the imaginary part of the solution is concerned — which, we recall, is our main interest here — the inclusion of this term is both essential and justified, as we shall later argue.

The approximate solutions (B.2) and (B.3) have a common validity range at  $u_1 < u \ll K/k$ , and thus can be matched with each other in this window. By also using the asymptotic behaviour of the modified Bessel functions, as valid for  $u \gg u_1$ , one finds

$$C_1 = \frac{2}{\sqrt{\pi}} C_3, \quad C_2 = 2\sqrt{\pi} C_4. \quad (\text{B.4})$$

(iii) For  $u \gg u_2$ , the WKB solution is similar to the one constructed in Sect. 4 and reads

$$\psi(u) \simeq \frac{C}{\sqrt{-V(u)}} \exp \left\{ i \int_{u_2}^u du' \sqrt{-V(u')} \right\}, \quad (\text{B.5})$$

where we have selected only the outgoing wave, i.e., the one propagating towards the black hole. (This corresponds to choosing  $c_5 = 0$  in Eq. (D.5).) The above coefficient  $C$  is the same as  $c_4$  in Eq. (D.5), but its precise value is irrelevant here (it would merely determine the normalization of the wave near  $u = 1$ , cf. Eqs. (D.2) and (D.7)). Rather, what matters is the relative normalization of the coefficients  $C_3$  and  $C_4$  in the solution (B.3) inside the barrier, which in turn is fixed by matching Eqs. (B.3) and (B.5) near  $u = u_2$ . This matching cannot be done by directly comparing these two solutions, as they have no overlap with each other. Yet, the proper matching procedure is standard in the WKB literature [71, 72] (this requires a study of the exact behaviour near  $u_2$ , which can be done by linearizing the potential and then recognizing the Airy equation), and here we shall simply list the result:

$$C_3 = \frac{C}{\sqrt{D}} e^{-i\pi/4}, \quad C_4 = \frac{i}{2} \sqrt{D} C e^{-i\pi/4} = \frac{i}{2} D C_3, \quad (\text{B.6})$$

where  $D$  is the WKB attenuation factor (in the usual context of quantum mechanics, this describes the decrease in the intensity  $|\Psi|^2$  of the wavefunction after passing the potential) :

$$D \equiv \exp \left\{ -2 \int_{u_1}^{u_2} du \sqrt{V(u)} \right\}. \quad (\text{B.7})$$

By comparing Eqs. (B.4) and (B.6) one finds

$$C_2 = i \frac{\pi}{2} D C_1, \quad (\text{B.8})$$

which implies the following behaviour for (B.2) near the boundary at  $u = 0$  (recall that  $\psi(u) \simeq \sqrt{u} a(u)$  for small  $u$ ) :

$$a(u) \simeq k^2 \mathcal{A}_L(0) \left[ \ln K^2 + (\ln u + 2\gamma) - i\pi D \right]. \quad (\text{B.9})$$

This is our main result here. It shows that, in the presence of a high potential barrier, the imaginary part of the solution near  $u = 0$  gets built via a *double-tunnel effect*. This is ‘double’ since the relative strength of the imaginary part versus the real part is  $D$ , and not  $\sqrt{D}$ . This result is in fact natural: this imaginary part is the feedback of the absorption taking place near  $u = 1$  on the gravitational perturbation at the Minkowski boundary. First, the incoming perturbation, which is purely real, has to cross the barrier to approach the black hole, then, after the scattering takes place near  $u = 1$ , the imaginary part thus generated in the solution must propagate backwards and cross the barrier once again, before being measured (in the form of DIS structure functions) at  $u = 0$ .

By using Eq. (B.9) together with the corresponding equation for the transverse sector, one can finally compute the DIS structure functions generated through tunneling in this low-energy (or low-temperature) regime. One thus finds quite similar expressions for the longitudinal ( $F_L = F_2 - 2xF_1$ ) and transverse ( $F_T = 2xF_1$ ) structure functions :

$$F_i \simeq \frac{N^2 Q^2 x}{32\pi^2} D_i \quad (i = L, T). \quad (\text{B.10})$$

It is easy to check that the integral in Eq. (B.7) is dominated by the region in  $u$  where the potential can be simplified to  $V(u) \simeq (K^2 - k^2 u^2)/u$ , which is the same as the potential (2.17) in the transverse sector and for  $u \ll 1$ . Then, the attenuation factor is essentially the same (to leading exponential accuracy) for both the longitudinal and the transverse waves, and can be estimated as

$$D \sim \exp \left\{ -c (K^3/k)^{1/2} \right\} \quad \text{with} \quad c = \frac{2\Gamma^2(1/4)}{3\sqrt{2\pi}}. \quad (\text{B.11})$$

This explains the estimates (5.1)–(5.2) for  $F_T$  and  $F_L$ .

Let us finally explain why, in the present context, we think that it was justified to keep the second term in the WKB solution (B.3). Generally, this term is discarded in applications of the WKB method [71, 72] since it is exponentially suppressed as compared to the first term there (recall that  $C_4 \propto DC_3$ , cf. (B.6)), and hence it is much smaller than the corrections to the prefactor in that first term, which are only power-suppressed (in this case, by rational powers of  $k/K^3$ ). However, in the present problem, the first exponential in (B.3) is matched onto the

real part,  $\propto C_1 K_0$ , of the solution at small  $u$ ; hence this large exponential term is strictly real, and so would be all the higher-order terms, neglected by the WKB approximation, which would correct its prefactor. Accordingly, the second exponential in (B.3) is the only one which can develop an imaginary part, and this imaginary part is therefore correct to WKB accuracy. To conclude, the WKB approximation cannot be trusted for the real part of the coefficient  $C_4$  in (B.3), but only for its imaginary part, which is the quantity of interest for us here.

### C. The operator product expansion at weak coupling

In this Appendix we shall show that, when computed to lowest-order in perturbation theory, the coefficient of the energy-momentum tensor in the operator product expansion (OPE) of the current-current correlator (2.1) is exactly the same as the corresponding coefficient in the strong-coupling limit, as implicitly computed in (3.20) (or in Eq. (A.5)). This nonrenormalization property reflects the high degree of supersymmetry of  $\mathcal{N} = 4$  SYM (see, e.g., [68]). In the perturbative calculation of the OPE to follow, we shall keep only the operators which mix with the energy-momentum tensor  $T_{\mu\nu}$ .

In  $\mathcal{N} = 4$  SYM, there are six scalars  $\phi_m$  in the vector representation of  $SO(6)$  and four Weyl fermions  $\psi_i$  in the fundamental representation of  $SU(4)$ . The  $\mathcal{R}$  symmetry current corresponding to the generator  $t^3 = \text{diag}(1/2, -1/2, 0, 0)$  is

$$J^\mu = \frac{1}{2}(\psi^1 \bar{\sigma}^\mu \psi^1 - \bar{\psi}^2 \bar{\sigma}^\mu \psi^2) + \frac{1}{2}(\phi_6 D^\mu \phi_5 - \phi_5 D^\mu \phi_6 + \phi_4 D^\mu \phi_3 - \phi_3 D^\mu \phi_4), \quad (\text{C.1})$$

where  $\bar{\sigma}^\mu = (1, -\vec{\sigma})$ ,  $\vec{\sigma}$  being the Pauli matrices. By contracting fields with free propagators, it is straightforward to derive the relevant part of the OPE:

$$\begin{aligned} & i \int d^4x e^{-iqx} J^\mu(x) J^\nu(0) \\ &= \frac{1}{Q^2} \left( \eta^{\mu\alpha} \eta^{\nu\beta} - \frac{q^\mu q^\alpha}{Q^2} \eta^{\nu\beta} - \eta^{\mu\alpha} \frac{q^\nu q^\beta}{Q^2} + \eta^{\mu\nu} \frac{q^\alpha q^\beta}{(Q^2)^2} \right) \left( \sum_{i=1,2} T_{\alpha\beta}^{\psi,i} + \sum_{m=3,4,5,6} T_{\alpha\beta}^{\phi,m} \right) \\ & - \frac{1}{(Q^2)^2} \left( \eta^{\mu\nu} - \frac{q^\mu q^\nu}{Q^2} \right) q^\alpha q^\beta \sum_{m=3,4,5,6} T_{\alpha\beta}^{\phi,m} + \dots \\ &= \frac{1}{Q^2} \left( \eta^{\mu\alpha} \eta^{\nu\beta} - \frac{q^\mu q^\alpha}{Q^2} \eta^{\nu\beta} - \eta^{\mu\alpha} \frac{q^\nu q^\beta}{Q^2} + \eta^{\mu\nu} \frac{q^\alpha q^\beta}{(Q^2)^2} \right) \left( \frac{1}{2} T_{\alpha\beta}^\psi + \frac{2}{3} T_{\alpha\beta}^\phi + (\text{nonsinglet terms}) \right) \\ & - \frac{1}{(Q^2)^2} \left( \eta^{\mu\nu} - \frac{q^\mu q^\nu}{Q^2} \right) q^\alpha q^\beta \left( \frac{2}{3} T_{\alpha\beta}^\phi + (\text{nonsinglet terms}) \right) + \dots \end{aligned} \quad (\text{C.2})$$

where in writing the second equality we have projected onto the  $SU(4)$  singlet operators and denoted

$$T_{\alpha\beta}^\phi \equiv \sum_{m=1}^6 T_{\alpha\beta}^{\phi,m} \equiv \sum_{m=1}^6 \phi_m i D_\alpha i D_\beta \phi_m \quad (\text{C.3})$$

and

$$T_{\alpha\beta}^\psi \equiv \sum_{i=1}^4 T_{\alpha\beta}^{\psi,i} \equiv \sum_{i=1}^4 \frac{i}{2} \bar{\psi}_i (\bar{\sigma}_\alpha D_\beta + \bar{\sigma}_\beta D_\alpha) \psi_i. \quad (\text{C.4})$$

These operators represent the energy–momentum tensors for scalar and fermion fields, respectively. Under renormalization, they mix with the total energy–momentum tensor, which also includes the respective operator for the gluon fields and reads

$$\begin{aligned} T_{\mu\nu} &= F_{\mu\lambda}^a F_{\nu}^{a\lambda} + \frac{i}{2} \sum_{i=1}^4 \bar{\psi}_i (\bar{\sigma}_\mu D_\nu + \bar{\sigma}_\nu D_\mu) \psi_i + \sum_{m=1}^6 D_\mu \phi_m D_\nu \phi_m + \dots \\ &\equiv T_{\mu\nu}^g + T_{\mu\nu}^\psi + T_{\mu\nu}^\phi. \end{aligned} \quad (\text{C.5})$$

Their mixing is governed by the anomalous dimension matrix for twist–two operators. The eigenoperators of the anomalous dimension matrix are [67]

$$T_I \equiv T^g + T^\psi + T^\phi, \quad T_{II} \equiv -2T^g + T^\psi + 2T^\phi, \quad T_{III} \equiv -T^g + 4T^\psi - 6T^\phi. \quad (\text{C.6})$$

The last two operators (unlike the former) have nonzero anomalous dimensions. After decomposing the operators which appear in the OPE (C.2) in terms of the above eigenvectors, i.e.,

$$\begin{aligned} \frac{1}{2}T^\psi + \frac{2}{3}T^\phi &= \frac{1}{3}T_I + \frac{1}{6}T_{II}, \\ \frac{2}{3}T^\phi &= \frac{2}{15}T_I + \frac{2}{21}T_{II} - \frac{2}{35}T_{III}, \end{aligned} \quad (\text{C.7})$$

we finally get

$$\begin{aligned} i \int d^4x e^{-iqx} J^\mu(x) J^\nu(0) &= \frac{1}{3Q^2} \left( \eta^{\mu\alpha} \eta^{\nu\beta} - \frac{q^\mu q^\alpha}{Q^2} \eta^{\nu\beta} - \eta^{\mu\alpha} \frac{q^\nu q^\beta}{Q^2} + \eta^{\mu\nu} \frac{q^\alpha q^\beta}{(Q^2)^2} \right) T_{\alpha\beta} \\ &\quad - \frac{2}{15(Q^2)^2} \left( \eta^{\mu\nu} - \frac{q^\mu q^\nu}{Q^2} \right) q^\alpha q^\beta T_{\alpha\beta} + \dots, \end{aligned} \quad (\text{C.8})$$

from which one can read the coefficients of  $T_{\mu\nu}$  in the OPE of the current–current correlator. Although explicitly obtained here via a lowest–order calculation in perturbation theory, these coefficients turn out to be exactly as those (indirectly) computed at strong coupling, in Sect. 3. To see that, let us specialize (A.4) to the high–energy regime, where

$$q^\alpha q^\beta T_{\alpha\beta} \approx (q^-)^2 T_{--} \approx 2q^2 T_{--}. \quad (\text{C.9})$$

and then take the thermal expectation value by using the expression (A.4) for the average energy momentum–tensor  $\Theta_{\mu\nu} \equiv \langle T_{\mu\nu} \rangle$  in a *strongly–coupled* SYM plasma. We thus obtain

$$\begin{aligned} i \int d^4x e^{-iqx} \langle J^\mu(x) J^\nu(0) \rangle &= \frac{\pi^2 N^2 T^4}{6Q^2} \left( n^\mu n^\nu - \frac{q \cdot n}{Q^2} q^\mu n^\nu - \frac{q \cdot n}{Q^2} q^\nu n^\mu + \frac{(q \cdot n)^2}{(Q^2)^2} \eta^{\mu\nu} \right) \\ &\quad - \frac{q^2 \pi^2 N^2 T^4}{15(Q^2)^2} \left( \eta^{\mu\nu} - \frac{q^\mu q^\nu}{Q^2} \right) \\ &= \frac{\pi^2 N^2 T^4}{6Q^2} \left( n_\mu - \frac{n \cdot q}{Q^2} q_\mu \right) \left( n_\nu - \frac{n \cdot q}{Q^2} q_\nu \right) + \frac{\pi^2 N^2 T^4 q^2}{10(Q^2)^2} \left( \eta^{\mu\nu} - \frac{q^\mu q^\nu}{Q^2} \right), \end{aligned} \quad (\text{C.10})$$

which is in full agreement with (3.20), as anticipated (recall that  $x = Q^2/2qT$ ). Normally, the OPE coefficients at strong coupling are extracted by studying 3- and 4–point correlation functions. Our method in Sect. 3 is more straightforward (though limited to the energy momentum tensor) in that we do not have to compute higher point functions, but only use the known value of  $\langle T_{\mu\nu} \rangle$  at finite temperature.

## D. High energy: the WKB approximation

In this Appendix, we shall construct approximate solutions to the gravitational wave equations in the high energy regime at  $k \gg K^3$ . We shall thus confirm and extend the results found in Sect. 4, which, we recall, were valid only for  $u \ll 1$ . The complete solutions will be obtained by matching three different approximations, valid for different values of  $u$ : the two limited solutions valid for  $u \ll 1$  and near  $u = 1$ , respectively, and the WKB solution valid in the intermediate region at  $0 < u \ll 1$ . In this construction, the outgoing-wave condition will be imposed near the black hole horizon at  $u = 1$ , in conformity with the original prescription in Refs. [61, 64].

The general solutions valid for  $u \ll 1$  have been already constructed in Sect. 4. In the longitudinal sector, this is given by Eq. (4.4), where the coefficient  $c_2$  is fixed by the boundary condition at  $u = 0$ , with the result shown in Eq. (4.5); as for  $c_1$ , this will be here obtained by matching onto the solution near  $u = 1$ , via the intermediate WKB solution.

Consider now the solution near the horizon. For  $k \gg K^3$  and  $u \simeq 1$ , Eq. (2.14) simplifies to

$$\psi'' + \frac{k^2}{4(1-u)^2} \psi = 0. \quad (\text{D.1})$$

The solution which obeys the right, outgoing-wave, behaviour near  $u = 1$  reads

$$\psi(u) = c_3(1-u)^{\frac{1}{2}(1-ik)}. \quad (\text{D.2})$$

(The second independent solution  $(1-u)^{\frac{1}{2}(1+ik)}$  must be rejected since it would describe a wave coming out from the horizon, i.e., a wave reflected by the black hole.)

Furthermore, in the intermediate region  $u_0 \ll u \ll 1$ , with  $u_0 = 1/(4k^2)^{1/3}$ , the ‘Schrödinger’ wave equation reads

$$\psi'' + \frac{k^2 u}{(1-u^2)^2} \psi = 0. \quad (\text{D.3})$$

The WKB solution has the standard structure  $\psi(u) = e^{i\sigma_0(u)}/\sqrt{|\sigma'_0|}$  with

$$\begin{aligned} \sigma_0(u) &= \int_0^u du' \sqrt{-V(u')} = \pm k \int_0^u du' \frac{\sqrt{u'}}{1-u'^2} \\ &= \pm \frac{k}{2} \left( \ln \frac{1+\sqrt{u}}{1-\sqrt{u}} - 2 \arctan \sqrt{u} \right). \end{aligned} \quad (\text{D.4})$$

Hence the general solution in this intermediate region reads

$$\begin{aligned} \psi(u) &= \sqrt{\frac{1-u^2}{k\sqrt{u}}} [c_4 F_k(u) + c_5 F_{-k}(u)], \\ F_k(u) &\equiv \left( \frac{1+\sqrt{u}}{1-\sqrt{u}} \right)^{ik/2} e^{-ik \arctan \sqrt{u}}. \end{aligned} \quad (\text{D.5})$$

We can now determine the unknown coefficients by matching the previous solutions in their common ranges of applicability. Comparing (D.2) and (D.5) near  $u = 1$  gives

$$c_5 = 0, \quad c_3 = c_4 \sqrt{\frac{2}{k}} e^{ik \ln 2 - i\pi k/4}. \quad (\text{D.6})$$

Then a comparison of (4.4) and (D.5) in the region  $u \ll 1$  but  $u \gg u_0$  — in this region  $\psi(u) \simeq \sqrt{u} a(u)$  and  $\xi \gg 1$ , so one can use the asymptotic expansions for the Bessel functions in Eq. (4.4) — gives, after simple calculations,

$$c_1 = -ic_2, \quad c_4 = \sqrt{\frac{3}{\pi}} c_2 e^{-3i\pi/4}. \quad (\text{D.7})$$

As anticipated, we have recovered the simple relation (4.6) between  $c_1$  and  $c_2$  which implies that already the small- $u$  solution, Eq. (4.4), is an outgoing wave, cf. Eq. (4.7).

Turning now to the transverse sector, where the small- $u$  solution was given in Eq. (4.9), we can similarly obtain the (outgoing-wave) solution near  $u = 1$  as

$$A_i(u) = c_3(1-u)^{-ik/2}, \quad (\text{D.8})$$

and the corresponding WKB solution as (compare to Eq. (D.5))

$$A_i = \frac{c_4}{\sqrt{k\sqrt{u}}} \left( \frac{1+\sqrt{u}}{1-\sqrt{u}} \right)^{ik/2} e^{-ik \arctan \sqrt{u}}. \quad (\text{D.9})$$

(We have anticipated that  $c_5$  is set to zero after matching onto Eq. (D.8).) The matching conditions then yield

$$c_1 = -ic_2, \quad c_3 = \frac{c_4}{\sqrt{q}} e^{ik \ln 2 - i\pi k/4}, \quad c_4 = \sqrt{3/\pi} c_1 \left( \frac{2k}{3} \right)^{1/3} e^{-5i\pi/12}. \quad (\text{D.10})$$

One finally gets the same result at small  $u$  as previously displayed in Eq. (4.10).

## References

- [1] E. Shuryak, *Why does the quark gluon plasma at RHIC behave as a nearly ideal fluid?*, *Prog. Part. Nucl. Phys.* **53** (2004) 273 [[arXiv:hep-ph/0312227](#)].
- [2] M. Gyulassy and L. McLerran, *New forms of QCD matter discovered at RHIC*, *Nucl. Phys.* **A 750** (2005) 30 [[arXiv:nucl-th/0405013](#)].
- [3] U. W. Heinz, *'RHIC serves the perfect fluid': Hydrodynamic flow of the QGP*, [[arXiv:nucl-th/0512051](#)].
- [4] B. Muller, *From Quark-Gluon Plasma to the Perfect Liquid*, [[arXiv:0710.3366 \[nucl-th\]](#)].
- [5] F. Karsch, *Properties of the quark gluon plasma: A lattice perspective*, *Nucl. Phys.* **A 783** (2007) 13 [[arXiv:hep-ph/0610024](#)].
- [6] G. Endrodi, Z. Fodor, S. D. Katz and K. K. Szabo, *The equation of state at high temperatures from lattice QCD*, [[arXiv:0710.4197 \[hep-lat\]](#)].
- [7] J. P. Blaizot, E. Iancu, and A. Rebhan, *Thermodynamics of the high-temperature quark-gluon plasma*, in *Quark-Gluon Plasma 3* (R. C. Hwa and X.-N. Wang, eds.). World Scientific, Singapore, 2003, [[arXiv:hep-ph/0303185](#)].
- [8] D. Teaney, *Effect of shear viscosity on spectra, elliptic flow, and Hanbury Brown-Twiss radii*, *Phys. Rev.* **C68** (2003) 034913 [[arXiv:nucl-th/0301099](#)].

- [9] K. H. Ackermann *et al.* [STAR Collaboration], *Elliptic flow in Au + Au collisions at  $s(NN)^{1/2} = 130$ -GeV*, *Phys. Rev. Lett.* **86** (2001) 402 [arXiv:nucl-ex/0009011].
- [10] K. Adcox *et al.* [PHENIX Collaboration], *Flow measurements via two-particle azimuthal correlations in Au + Au collisions at  $s(NN)^{1/2} = 130$ -GeV*, *Phys. Rev. Lett.* **89** (2002) 212301 [arXiv:nucl-ex/0204005].
- [11] S. S. Adler *et al.* [PHENIX Collaboration], *Suppressed  $\pi^0$  production at large transverse momentum in central Au + Au collisions at  $s(NN)^{1/2} = 200$ -GeV*, *Phys. Rev. Lett.* **91** (2003) 072301 [arXiv:nucl-ex/0304022].
- [12] J. Adams *et al.* [STAR Collaboration], *Transverse momentum and collision energy dependence of high  $p(T)$  hadron suppression in Au + Au collisions at ultrarelativistic energies*, *Phys. Rev. Lett.* **91** (2003) 172302 [arXiv:nucl-ex/0305015].
- [13] K. J. Eskola, H. Honkanen, C. A. Salgado and U. A. Wiedemann, *The fragility of high- $p(T)$  hadron spectra as a hard probe*, *Nucl. Phys.* **A747** (2005) 511 [arXiv:hep-ph/0406319].
- [14] A. Dainese, C. Loizides and G. Paic, *Leading-particle suppression in high energy nucleus nucleus collisions*, *Eur. Phys. J.* **C38** (2005) 461 [arXiv:hep-ph/0406201].
- [15] R. Baier, Y. L. Dokshitzer, A. H. Mueller, S. Peigne and D. Schiff, *Radiative energy loss of high energy quarks and gluons in a finite-volume quark-gluon plasma*, *Nucl. Phys.* **B483** (1997) 291 [arXiv:hep-ph/9607355].
- [16] R. Baier, D. Schiff and B. G. Zakharov, *Energy loss in perturbative QCD*, *Ann. Rev. Nucl. Part. Sci.* **50** (2000) 37 [arXiv:hep-ph/0002198].
- [17] R. Baier and D. Schiff, *Deciphering the properties of the medium produced in heavy ion collisions at RHIC by a  $p$ QCD analysis of quenched large  $p(T)$   $\pi^0$  spectra*, *JHEP* **0609** (2006) 059 [arXiv:hep-ph/0605183].
- [18] T. Umeda, K. Nomura and H. Matsufuru, *Charmonium at finite temperature in quenched lattice QCD*, *Eur. Phys. J.* **C 39S1** (2005) 9 [arXiv:hep-lat/0211003].
- [19] M. Asakawa and T. Hatsuda,  *$J/\psi$  and  $\eta/c$  in the deconfined plasma from lattice QCD*, *Phys. Rev. Lett.* **92** (2004) 012001 [arXiv:hep-lat/0308034].
- [20] S. Datta, F. Karsch, P. Petreczky and I. Wetzorke, *Behavior of charmonium systems after deconfinement*, *Phys. Rev.* **D 69** (2004) 094507 [arXiv:hep-lat/0312037].
- [21] G. Aarts, C. Allton, M. B. Oktay, M. Peardon and J. I. Skullerud, *Charmonium at high temperature in two-flavor QCD*, [arXiv:0705.2198 [hep-lat]].
- [22] J. P. Blaizot, E. Iancu, and A. Rebhan, *Approximately self-consistent resummations for the thermodynamics of the quark-gluon plasma: Entropy and density*, *Phys. Rev.* **D63** (2001) 065003, [arXiv:hep-ph/0005003].
- [23] J. O. Andersen, E. Braaten, E. Petitgirard, and M. Strickland, *HTL perturbation theory to two loops*, *Phys. Rev.* **D66** (2002) 085016, [arXiv:hep-ph/0205085].
- [24] K. Kajantie, M. Laine, K. Rummukainen and Y. Schroder, *The pressure of hot QCD up to  $g^{*6} \ln(1/g)$* , *Phys. Rev.* **D67** (2003) 105008 [arXiv:hep-ph/0211321].
- [25] S. Caron-Huot and G. D. Moore, *Heavy quark diffusion in perturbative QCD at next-to-leading order*, [arXiv:0710.3366 [hep-ph]].

- [26] J. M. Maldacena, *The large  $N$  limit of superconformal field theories and supergravity*, *Adv. Theor. Math. Phys.* **2** (1998) 231 [arXiv:hep-th/9711200];  
 S. S. Gubser, I. R. Klebanov and A. M. Polyakov, *Gauge theory correlators from non-critical string theory*, *Phys. Lett.* **B 428** (1998) 105 [arXiv:hep-th/9802109];  
 E. Witten, *Anti-de Sitter space and holography*, *Adv. Theor. Math. Phys.* **2** (1998) 253 [arXiv:hep-th/9802150].
- [27] S. S. Gubser, I. R. Klebanov and A. W. Peet, *Entropy and Temperature of Black 3-Branes*, *Phys. Rev.* **D 54** (1996) 3915 [arXiv:hep-th/9602135].
- [28] E. Witten, *Anti-de Sitter space, thermal phase transition, and confinement in gauge theories*, *Adv. Theor. Math. Phys.* **2** (1998) 505 [arXiv:hep-th/9803131].
- [29] G. Policastro, D. T. Son and A. O. Starinets, *The shear viscosity of strongly coupled  $N = 4$  supersymmetric Yang-Mills plasma*, *Phys. Rev. Lett.* **87** (2001) 081601 [arXiv:hep-th/0104066].
- [30] G. Policastro, D. T. Son and A. O. Starinets, *From AdS/CFT correspondence to hydrodynamics*, *JHEP* **0209** (2002) 043 [arXiv:hep-th/0205052].
- [31] H. Liu, K. Rajagopal and U. A. Wiedemann, *Calculating the jet quenching parameter from AdS/CFT*, *Phys. Rev. Lett.* **97** (2006) 182301 [arXiv:hep-ph/0605178].
- [32] N. Armesto, J. D. Edelstein and J. Mas, *Jet quenching at finite 't Hooft coupling and chemical potential from AdS/CFT*, *JHEP* **0609** (2006) 039 [arXiv:hep-ph/0606245].
- [33] F. L. Lin and T. Matsuo, *Jet quenching parameter in medium with chemical potential from AdS/CFT*, *Phys. Lett.* **B 641** (2006) 45 [arXiv:hep-th/0606136].
- [34] H. Liu, K. Rajagopal and U. A. Wiedemann, *Wilson loops in heavy ion collisions and their calculation in AdS/CFT*, *JHEP* **0703** (2007) 066 [arXiv:hep-ph/0612168].
- [35] S. S. Gubser, *Drag force in AdS/CFT*, *Phys. Rev.* **D 74** (2006) 126005 [arXiv:hep-th/0605182].
- [36] C. P. Herzog, A. Karch, P. Kovtun, C. Kozcaz and L. G. Yaffe, *Energy loss of a heavy quark moving through  $N = 4$  supersymmetric Yang-Mills plasma*, *JHEP* **0607** (2006) 013 [arXiv:hep-th/0605158].
- [37] C. P. Herzog, *Energy loss of heavy quarks from asymptotically AdS geometries*, *JHEP* **0609** (2006) 032 [arXiv:hep-th/0605191].
- [38] E. Caceres and A. Guijosa, *Drag force in charged  $N = 4$  SYM plasma*, *JHEP* **0611** (2006) 077 [arXiv:hep-th/0605235].
- [39] K. Peeters, J. Sonnenschein and M. Zamaklar, *Holographic melting and related properties of mesons in a quark gluon plasma*, *Phys. Rev.* **D74** (2006) 106008 [arXiv:hep-th/0606195].
- [40] H. Liu, K. Rajagopal and U. A. Wiedemann, *An AdS/CFT calculation of screening in a hot wind*, *Phys. Rev. Lett.* **98** (2007) 182301 [arXiv:hep-ph/0607062].
- [41] M. Chernicoff, J. A. Garcia and A. Guijosa, *The energy of a moving quark-antiquark pair in an  $N = 4$  SYM plasma*, *JHEP* **0609** (2006) 068 [arXiv:hep-th/0607089].
- [42] E. Caceres, M. Natsuume and T. Okamura, *Screening length in plasma winds*, *JHEP* **0610** (2006) 011 [arXiv:hep-th/0607233].
- [43] P. C. Argyres, M. Edalati and J. F. Vazquez-Poritz, *No-drag string configurations for steadily moving quark-antiquark pairs in a thermal bath*, *JHEP* **0701** (2007) 105 [arXiv:hep-th/0608118].

- [44] S. D. Avramis, K. Sfetsos and D. Zoakos, *On the velocity and chemical-potential dependence of the heavy-quark interaction in  $N = 4$  SYM plasmas,* *Phys. Rev.* **D75** (2007) 025009 [arXiv:hep-th/0609079].
- [45] J. Casalderrey-Solana and D. Teaney, *Heavy quark diffusion in strongly coupled  $N = 4$  Yang Mills,* *Phys. Rev.* **D 74** (2006) 085012 [arXiv:hep-ph/0605199].
- [46] J. Casalderrey-Solana and D. Teaney, *Transverse momentum broadening of a fast quark in a  $N = 4$  Yang Mills plasma,* *JHEP* **0704** (2007) 039 [arXiv:hep-th/0701123].
- [47] S. S. Gubser, S. S. Pufu and A. Yarom, *Energy disturbances due to a moving quark from gauge-string duality,* *JHEP* **0709** (2007) 108 [arXiv:0706.0213 [hep-th]].
- [48] P. M. Chesler and L. G. Yaffe, *The wake of a quark moving through a strongly-coupled  $\mathcal{N} = 4$  supersymmetric Yang-Mills plasma,* *Phys. Rev. Lett.* **99** (2007) 152001 [arXiv:0706.0368 [hep-th]].
- [49] D. Bak, A. Karch and L. G. Yaffe, *Debye screening in strongly coupled  $N=4$  supersymmetric Yang-Mills plasma,* *JHEP* **0708** (2007) 049 [arXiv:0705.0994 [hep-th]].
- [50] I. Amado, C. Hoyos, K. Landsteiner and S. Montero, *Absorption Lengths in the Holographic Plasma,* *JHEP* **0709** (2007) 057 [arXiv:0706.2750 [hep-th]].
- [51] S. Caron-Huot, P. Kovtun, G. D. Moore, A. Starinets and L. G. Yaffe, *Photon and dilepton production in supersymmetric Yang-Mills plasma,* *JHEP* **0612** (2006) 015 [arXiv:hep-th/0607237].
- [52] R. A. Janik and R. Peschanski, *Asymptotic perfect fluid dynamics as a consequence of AdS/CFT,* *Phys. Rev.* **D 73** (2006) 045013 [arXiv:hep-th/0512162].
- [53] S. Nakamura and S. J. Sin, *A holographic dual of hydrodynamics,* *JHEP* **0609** (2006) 020 [arXiv:hep-th/0607123].
- [54] Y. V. Kovchegov and A. Taliotis, *Early time dynamics in heavy ion collisions from AdS/CFT correspondence,* *Phys. Rev.* **C 76** (2007) 014905 [arXiv:0705.1234 [hep-ph]].
- [55] K. Kajantie, J. Louko and T. Tahkokallio, *The gravity dual of 1+1 dimensional Bjorken expansion,* [arXiv:0705.1791 [hep-th]].
- [56] J.-P. Blaizot and E. Iancu, *The quark-gluon plasma: Collective dynamics and hard thermal loops,* *Phys. Rept.* **359** (2002) 355–528, [hep-ph/0101103].
- [57] J. Polchinski and M. J. Strassler, *Deep inelastic scattering and gauge/string duality,* *JHEP* **0305** (2003) 012 [arXiv:hep-th/0209211].
- [58] Y. Hatta, E. Iancu and A. H. Mueller, *Deep inelastic scattering at strong coupling from gauge/string duality: the saturation line,* [arXiv:0710.2148 [hep-th]].
- [59] A. H. Mueller, *Parton Saturation—An Overview, QCD Perspectives on Hot and Dense Matter* (J.-P. Blaizot and E. Iancu, eds.), NATO Science Series, Kluwer, 2002, [arXiv:hep-ph/0111244];  
E. Iancu and R. Venugopalan, *The Color Glass Condensate and High Energy Scattering in QCD,* in *Quark-Gluon Plasma 3* (R. C. Hwa and X.-N. Wang, eds.). World Scientific, Singapore, 2003, [arXiv:hep-ph/0303204].
- [60] I. R. Klebanov, *World-volume approach to absorption by non-dilatonic branes,* *Nucl. Phys.* **B 496** (1997) 231 [arXiv:hep-th/9702076].
- [61] D. T. Son and A. O. Starinets, *Minkowski-space correlators in AdS/CFT correspondence: Recipe and applications,* *JHEP* **0209** (2002) 042 [arXiv:hep-th/0205051].

- [62] C. P. Herzog and D. T. Son, *Schwinger-Keldysh propagators from AdS/CFT correspondence*, *JHEP* **0303** (2003) 046 [[arXiv:hep-th/0212072](#)].
- [63] D. Teaney, *Finite temperature spectral densities of momentum and R-charge correlators in  $N = 4$  Yang Mills theory*, *Phys. Rev. D* **74** (2006) 045025 [[arXiv:hep-ph/0602044](#)].
- [64] D. T. Son and A. O. Starinets, *Viscosity, Black Holes, and Quantum Field Theory*. [[arXiv:0704.0240](#) [[hep-th](#)]].
- [65] D. Anselmi, D. Z. Freedman, M. T. Grisaru and A. A. Johansen, *Nonperturbative formulas for central functions of supersymmetric gauge theories*, *Nucl. Phys. B* **526** (1998) 543 [[arXiv:hep-th/9708042](#)].
- [66] M. Abramowitz and I. A. Stegun, *Handbook of Mathematical functions*, Dover, New York (1972), pp 447.
- [67] D. Anselmi, *The  $N = 4$  quantum conformal algebra*, *Nucl. Phys. B* **541** (1999) 369 [[arXiv:hep-th/9809192](#)].
- [68] G. Arutyunov, S. Frolov and A. C. Petkou, *Operator product expansion of the lowest weight CPOs in  $N = 4$  SYM(4) at strong coupling*, *Nucl. Phys. B* **586** (2000) 547 [*Erratum-ibid.* **B 609** (2001) 539] [[arXiv:hep-th/0005182](#)].
- [69] G. Chalmers, H. Nastase, K. Schalm and R. Siebelink, *R-current correlators in  $N = 4$  super Yang-Mills theory from anti-de Sitter supergravity*, *Nucl. Phys. B* **540** (1999) 247 [[arXiv:hep-th/9805105](#)].
- [70] G. R. Farrar, H. Liu, L. L. Frankfurt and M. I. Strikman, *Transparency in Nuclear Quasieexclusive Processes with Large Momentum Transfer*, *Phys. Rev. Lett.* **61** (1988) 686.
- [71] L. D. Landau and L. M. Lifshitz, *Quantum Mechanics: Non-Relativistic Theory* Butterworth-Heinemann, 1981.
- [72] C. M. Bender and S. A. Orszag, *Advanced mathematical methods for scientists and engineers*, Second Edition, McGraw-Hill, Singapore, 1984.